Experimental Access to the Molecular and Electronic Structures of Organo-f-Element Complexes by NMR Spectroscopy

WERNER JAHN, KENAN YÜNLÜ, WOLFGANG OROSCHIN, HANS-DIETER AMBERGER and R. DIETER FISCHER*

Institut für Anorganische und Angewandte Chemie der Universität Hamburg, Martin-Luther-King-Platz 6, D-2000 Hamburg 13, F.R.G.

Received November 7, 1983**

The main objective of this survey is to demonstrate that by extensive assessment of variable temperature ^1H NMR data obtained on paramagnetic f-element complexes in solution, not only valuable information on details of the molecular structure, but also on the electronic structure may be deduced. One of the most informative quantities to arrive at is the paramagnetic anisotropy term, $\chi_{\parallel} - \chi_{\perp}$, of axially symmetric molecules from which, if the bulk susceptibility $\bar{\chi}$ is also known, the crystal-field sensitive parameters $\chi_{\parallel}$ and $\chi_{\perp}$ can be derived.

The majority of the examples considered belong to the widely studied type $[Cp_3{}^fML_n]^q$ ($Cp = \eta^5$-C_5H_4R); ^fM = Pr(III), Nd(III), Yb(III) and U(IV); n = 0, 1 and 2; q = 0 or −1) and to the uranocene family. The survey also includes the two sub-classes of novel anionic complexes $[Cp_3LnL]^-$ and $([Cp_3Ln)_2(\mu\text{-}L)]^-$, respectively, and different isomers of the general composition $[Cp_3UXY]^q$ (Ln = lanthanoid).

†Dedicated to Prof. Dr. Dr. h.c. mult. E. O. Fischer on the occasion of his 65th birthday (Nov. 10, 1983).

*Author to whom correspondence should be addressed.

**Manuscript based on a Plenary Lecture presented by R.D.F. on the occasion of the 1st ICLA, Venice, Italy, Sept. 5–10, 1983.

Introduction

While information on the electronic structure of f-element compounds may be obtained from experimental techniques similar to those that have been established for the investigation of d-transition element compounds, some physico-chemical methods have recently proved to be of superior value for the systematic examination of f-element compounds, or at least, for a few representative families thereof (Table I). Most of the latter methods have focused particularly on the properties of energetically rather low-lying electronic states (crystal field, or CF- states) and on the very specific variation of the magnetic properties of discrete states, and thermally-populated ensembles of different states, respectively.

Organometallic complexes are frequently soluble in coordinatively inert solvents and, owing to the presence of nuclei such as ^1H and ^{13}C, and sometimes of ^{31}P, ^{11}B etc. as well, offer the almost unique possibility of detailed NMR spectroscopic studies of dissolved, practically free molecules. Since the spectacular evolution of versatile analytical techniques involving lanthanide-induced NMR shift reagents [5] it has become widely known that well-observable

TABLE I. Valuable Experimental Techniques for Studies of the Electronic Structures of f- (and d-) Transition Metal Compounds.

Method	Optimal state of sample	Optimal temp. of sample	Energies of relevant excited states
NIR/VIS-spectroscopy (absorption)	solid/soln.	variable temp.	$\geq$ *ca.* 4000 cm^{-1}
Luminescence spectroscopy[c]	solid/(soln.)	variable temp.	0–*ca.* 5000 cm^{-1}
(F)IR-spectroscopy[b,d]	solid	$\ll$ RT	*ca.* 20–5000 cm^{-1}
Electronic Raman scattering[a]	solid	$\ll$ RT	*ca.* 20–7000 cm^{-1}
MCD-spectroscopy (NIR/VIS/UV)	soln.	variable temp.	$>$ *ca.* 5000 cm^{-1}
EPR-spectroscopy	solid	$\ll$ RT	0–*ca.* 50 cm^{-1}
Bulk magnetic susceptibility	solid	variable temp.	0–*ca.* 1000 cm^{-1}
Bulk magnetic susceptibility	soln. (by NMR)	variable temp.	0–*ca.* 1000 cm^{-1}
Magnet. susceptibility tensor components	solid	variable temp.	0–*ca.* 1000 cm^{-1}
Magnet. susceptibility tensor components	soln. (by NMR)	variable temp.	0–*ca.* 1000 cm^{-1}

[a] See Ref. [1]. [b] See Ref. [2]. [c] See Ref. [3]. [d] See Ref. [4a]. [e] See Ref. [4b].

0020-1693/84/$3.00

NMR shifts of paramagnetic metal ion complexes may equally well be evaluated in view of the (topological) molecular and the (CF-determined) electronic structure [6]. As a general rule, detailed analyses of the NMR data of paramagnetic samples will be most promising in either direction when the molecular structure of the complex of interest, or at least the average crystal field experienced by the central metal ion, is of axial symmetry [6, 7].

The present survey is therefore confined to some instructive aspects of ^{1}H NMR spectroscopic studies of the (so far) most extensively described class of axially (or, at least, pseudo-axially) symmetric organometallics of the f-elements. Common to all members of this class is the general composition $[Cp_3'^{f}ML_n]^q$ in which the appearance of one trigonal rotational axis is throughout accomplished by the presence of three equivalent η^5-coordinated cyclopentadienyl ligands (Scheme 1). Important variables

General complex type: $[Cp_3'^{f}ML_n]^q$

Cp' = η^5-C_5H_4R (R = *e.g.* H, CH_3, $Si(CH_3)_3$)
^fM = Ln(III) or An(IV)
(Ln = *e.g.* La, Pr, Nd, Yb etc.; An = U, Np, Pu)
L = uncharged or anionic Lewis base
n = 0, 1/2, 1, 2
q = 0, +1, −1

Scheme 1. General composition, and specification of variable components, of tris(cyclopentadienyl) complexes of f-metal ions.

that will affect the ^{1}H NMR spectra are the nature of the central metal ion, the nature and electric charge of the extra ligand(s) L (and L'), the number of extra ligands per metal ion, and the nature of the Cp' ring substituent R that occasionally replaces one hydrogen atom of each η^5-C_5H_5 ligand. Next to the class of $[Cp_3'^{f}ML_n]^q$ systems, derivatives of the apparently unique class of sandwich complexes involving a central f-metal ion, $[(\eta^8\text{-}C_8H_8)_2{}^{f}M]^q$, are axially symmetric systems. So far, however, extensive NMR studies have only been focused on ring-substituted uranocene derivatives ($^fM = U^{IV}$, q = 0) [8, 9] and will only be considered briefly here.

Recalling that NMR spectroscopy of paramagnetic samples belongs (like *e.g.* paramagnetic susceptibility studies and MCD spectroscopy) to the increasing diversity of magnetochemical techniques, it should become evident that careful studies of the temperature dependence of the NMR spectra play an essential role for any meaningful further evaluation of experimental data. Rapid chemical equilibria between different paramagnetic species (by inter- or intramolecular pathways) may cause (particularly in solution) experimental features substantially different from the expectation focused on one singular, nonreacting molecular species. In terms of practical assessment, this means that plots between 200–300 K of the observed NMR shift and the reciprocal temperature may deviate from linearity (and hence from the familiar 'Curie-Weiss-rule') just for 'chemical', and not, primarily, for structural or electronic reasons.

Graphs involving the NMR shifts of paramagnetic samples may adopt either the familiar 'chemical shift' δ referring all displacements as usual to the internal standard tetramethylsilane (TMS), or, as soon as any assessment toward the electronic structure is intended, the so-called isotropic shift Δ^{iso}. This latter quantity is referred to an individually chosen internal standard containing the nucleus of the paramagnetic sample in question in a completely diamagnetic environment (*e.g.* for C_5H_5-protons of paramagnetic $(C_5H_5)_3LnL$-complexes, $(C_5H_5)_3La\cdot THF$ would be an appropriate diamagnetic standard). Unlike in most cases of applying a paramagnetic shift reagent to merely structural problems, it is most essential to choose for Δ^{iso} the magnetochemically relevant sign. In the following, Δ^{iso} is always assumed positive if δ^{para} occurs at a higher magnetic field strength (of the spectrometer) than δ^{dia} (and *vice versa*). The general strategy typical of the evaluation of NMR-data of structurally suitable paramagnetic samples with respect to the electronic structure is depicted in Scheme 2.

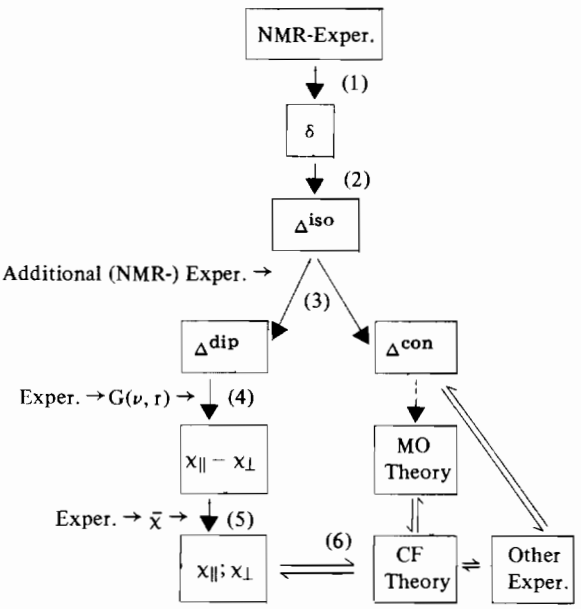

Scheme 2. Schematic view of the applicability of NMR-data for magnetochemical and CF-theoretical assessments (G(ν, r) = geometry factor, *vide infra*).

Most generally, Δ^{iso} is composed of two different terms, Δ^{dip} and Δ^{con},

$$\Delta^{iso} = \Delta^{dip} + \Delta^{con} \quad (1)$$

the so-called dipolar (or 'pseudocontact') term Δ^{dip} accounting for through-space interactions between the magnetic moment of the nucleus of interest and the

(dipolar) magnetic moment of the unpaired f-electrons most frequently assumed to be localized on the central metal ion. The so-called (Fermi) contact term Δ^{con} is non-vanishing if any (usually minor) fraction of the free electron spin density resides on the nucleus considered. All attempts to conclusively correlate Δ^{con} with quantities relevant of chemical bonding, in particular of the degree of covalency [10], have so far suffered from the ambiguity of the models envisaged for the spin transfer, and the high degree of sophistication of the quantum chemical computations afforded to verify Δ^{con} theoretically.

Experience has confirmed that Δ^{con} usually attenuates rapidly with the number of (single) bonds between the nucleus in question and the paramagnetic centre, allowing in fortunate situations the assumption: $\Delta^{dip} \approx \Delta^{iso}$ already for nuclei of atoms separated from the (lanthanide) ion by at least three bonds. This circumstance turns out to be most helpful to overcome step 3 of Scheme 2. While for step 4 the knowledge of two distinct structural parameters is needed, step 5 is performed by accounting the average bulk magnetic susceptibility $\bar{\chi} = \frac{1}{3}(\chi_{\parallel} + 2\chi_{\perp})$, usually obtained from conventional magnetic susceptibility studies on polycrystalline samples. In principle, however, $\bar{\chi}$ may likewise be obtained from NMR studies of the dissolved sample referring in this case the solvent signal(s) of the paramagnetic solution to the corresponding resonance of the same solvent chosen as the external standard [11].

Ligand (L) Resonances of $[Cp_3'^{f}ML_n]^q$-Systems with n = 1, q = 0 and R = H

Historically, this particular class of f-element organometallics involving both $^fM = U^{IV}$ (and L = a halide or pseudohalide anion) and ^fM = *e.g.* Pr^{III}, Eu^{III} and Yb^{III} (and L an uncharged Lewis base) has been subjected to extensive ^1H NMR investigations since *ca.* 1970 [12]. Thus it has been demonstrated that below *ca.* −50 °C the corresponding 1:1 adducts with L = cyclohexylisocyanide and $^fM = Ce^{III}$, Pr^{III}, Nd^{III} and Eu^{III} give rise to ^1H NMR spectra of the non-rapidly [13] interconverting two conformers in which the axially symmetric $Cp_3{}^fMCN$-moiety is bonded to an axial and equatorial position, respectively, of the cyclohexyl group (Fig. 1) [14, 15]. The plots of the respective isotropic shifts Δ^{iso} of the 12 to 14 cyclohexyl protons of different spatial positions (relative to the central metal ion) versus their individual geometric factors G_i (quantifying these different spatial positions [17]) correspond for each of the complexes with ^fM = Ce, Pr, Nd and Eu to a straight line, clearly starting at the origin of the coordinate system [15] (see also Fig. 1). The structural parameters used to compute the G_i-values are essentially in good accord with an X-ray diffraction study

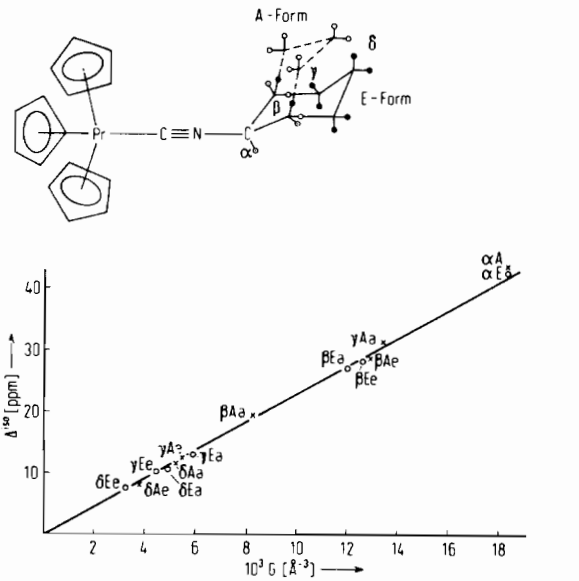

Fig. 1. Schematic description of the two conformers of $Cp_3PrCNC_6H_{11}$ (above), and Δ_i^{iso}-*vs*-G_i plot (−70 °C) of all differently oriented cyclohexyl H-atoms (below). From ref. [16].

of the Pr-complex [18]; however, as only one conformer with a 'flattened' C_6H_{11}-chair is realized in the solid state, the—as yet hypothetical—^1H NMR spectra of the solid complex would differ considerably from the solution spectra.

From the clear proportionality of Δ_i^{iso} and G_i we suggest that, with the only exception of the α-proton of the Eu-complex [19], Δ^{con} is negligible even in case of the α-protons of the complexes with ^fM = Ce–Nd. Furthermore, the slopes of the four straight lines are directly proportional to the quantity $\chi_{\parallel} - \chi_{\perp}$ (eqn. 2, [12]) at the respective temperature ($\chi_{\parallel} - \chi_{\perp}$ being <0 for a positive slope, and *vice versa*).

$$\Delta^{dip} = -G/3N_L \cdot (\chi_{\parallel} - \chi_{\perp}) \qquad (2)$$

More recent results with M = Pr and Nd have shown that replacement of the ligand L = CNC_6H_{11} by the isoelectronic systems $NCCH_3$ and $NCBH_3^-$, respectively, gives rise to isotropic ligand ^1H NMR shifts almost unchanged with respect to those of the α-proton of the CNC_6H_{11} ligand (Fig. 2). In accordance with the expectation that in case of $\Delta^{dip} \approx \Delta^{iso}$ closely resembling δ-*vs*-T^{-1} plots should result for all nuclei of comparable geometric factors, the three different samples: $Cp_3PrNCCH_3$ in CD_2Cl_2, $Cp_3Pr/[NBu_4^n]NCBH_3$ (1:1) in CD_2Cl_2 and $Cp_3PrCNC_6H_{11}$ in toluene-d_8 in fact give rise to similar, essentially linear, δ-*vs*-T^{-1} plots. This result confirms both the assumption of a 1:1 adduct with N-bonded $NCBH_3^-$, and the earlier suggestion of a negligibly-small contact contribution, Δ_α^{con}, despite the π-bonding involved in the NC triple bonds. On the

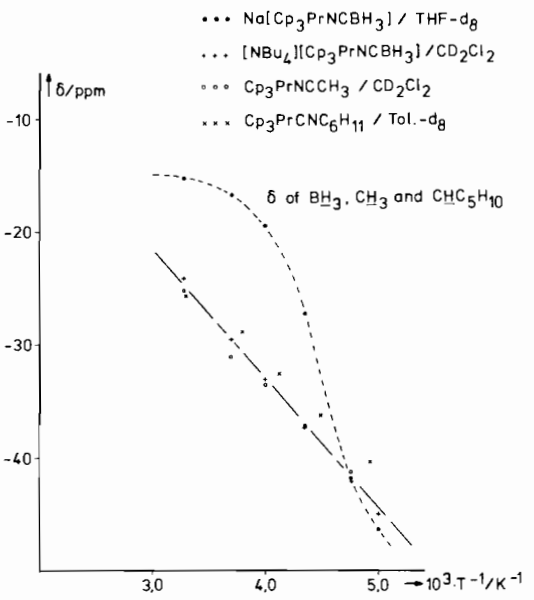

Fig. 2. δ-*vs*-T^{-1} plots of CH_3-protons (L = CH_3CN), BH_3-protons (L = $NCBH_3^-$) and α-H atoms of C_6H_{11} (L = CNC_6H_{11}), respectively, of various adducts Cp_3PrL (data of C_6H_{11}-resonances from ref. [14]).

other hand, replacement of the practically non-coordinating solvent CD_2Cl_2 by THF-d_8 (and of the counter-cation $[NBu_4^n]^+$ by Na^+) leads to a completely different δ-*vs*-T^{-1} curve of sigmoid shape, suggesting that the appearance of the resulting plot is now influenced by the temperature-dependent equilibrium (3)

$$[Cp_3PrNCBH_3]^- + THF \rightleftharpoons Cp_3PrTHF + NCBH_3^- \quad (3)$$

Another instructive example of an essentially sigmoid δ-*vs*-T^{-1} curve reflecting equilibrium-sensitive NMR features, and which is very rapid on the NMR time-scale, involves the addition of a Lewis base L to the Lewis acid Cp_3UF [20]

$$[Cp_3UF]_2 + 2L \overset{\text{toluene-}d_8}{\rightleftharpoons} 2Cp_3U(L)F \text{ (L = pyridine or THF)} \quad (4)$$

Returning to the strategy depicted in Scheme 2, a good estimate of the average geometry factor G of the α-H atoms is easily arrived at on the basis of the molecular structure of the complex $Cp_3PrCNC_6H_{11}$ [18]. A corresponding estimate of G is facile to make for the methyl H-atoms of the related γ-picoline adduct. Table II then shows that very similar, negative values result for the quantity $\chi_\parallel - \chi_\perp$, in spite of the rather different 'test ligands' L. Moreover, by adopting the average $(\chi_\parallel - \chi_\perp)$-values of Table II for a further assessment of the observed ligand proton resonances of some adducts Cp_3PrL with simple carboxylic esters, an optimal graphical fit of the Δ^{dip}-values and the corresponding geometry factors G_i is only achieved for a COPr-angle of 150 ± 10°. This value is in excellent accord with the X-ray crystallographically confirmed value for the COTi-angle of 152.1° in the adduct $[TiCl_4 \cdot CH_3COOC_2H_5]_2$ [21]. Hence, the 1:1 adducts of Cp_3Pr with various different uncharged Lewis bases (including also the $NCBH_3$-anion) may display (at least at room temperature) a very similar magnetic anisotropy term, $\chi_\parallel - \chi_\perp$.

Adopting now for step 4 of Scheme 2 the experimental paramagnetic bulk susceptibility, $\bar{\chi}$, of the complex $Cp_3PrCNC_6H_{11}$ [22], the individual values of $\chi_\parallel$(exp.) and $\chi_\perp$(exp.) for the temperature range 200–300 K become available. In Fig. 3 the resulting pair of χ^{-1}(exp.)-*vs*-T is compared with the pair of independently-calculated χ^{-1}(calc.)-*vs*-T plots, the calculation of $\chi_\parallel$, $\chi_\perp$ and $\bar{\chi}$ being based on a complete set of crystal field parameters $\langle r^n \rangle A_n^m = B_n^m$ deduced from combined NIR/VIS- and MCD-studies of $Cp_3PrCNC_6H_{11}$ at different temperatures [23]. It is noteworthy that $\chi_\perp(\text{exp.})^{-1}$ and $\chi_\perp(\text{calc.})^{-1}$ lie surprisingly close together, and their plots have the same slopes, while numerically $\chi_\parallel(\text{exp.})^{-1}$ and $\chi_\parallel(\text{calc.})^{-1}$ show somewhat larger differences, but the corresponding plots nevertheless display a similar kind of temperature dependence.

TABLE II. Magnetic Anisotropy, $\chi_\parallel - \chi_\perp$, of Various Cp_3PrL-Systems at Room Temperature, Derived from NMR-Data.

Complex	Δ^{dip} (in ppm)	G(CH_3) (in cm^{-3})	$\chi_\parallel - \chi_\perp$ (in $cm^3\ mol^{-1}$)
$Cp_3PrNCCH_3$	27.4	$1.072 \cdot 10^{22}$	$-4619 \cdot 10^{-6}$
$[Cp_3PrNCBH_3]^-$	24.0	$0.944 \cdot 10^{22}$	$-4592 \cdot 10^{-6}$
$Cp_3PrCNCHC_5H_{10}$	27.0	$1.072 \cdot 10^{22}$	$-4550 \cdot 10^{-6}$
$Cp_3PrNC_5H_4CH_3$[c]	11.4	$0.474 \cdot 10^{22}$	$-4349 \cdot 10^{-6}$
$Cp_3PrOC(CH_3)OCH_3$	25.1 (calc. 25.9)[a] 23.7 (calc. 24.4)[b]	$1.09 \cdot 10^{22}$ $1.07 \cdot 10^{22}$	$-4300 \cdot 10^{-6}$ (assumed)

[a] For CH_3. [b] For OCH_3. [c] L = 4-methylpyridine.

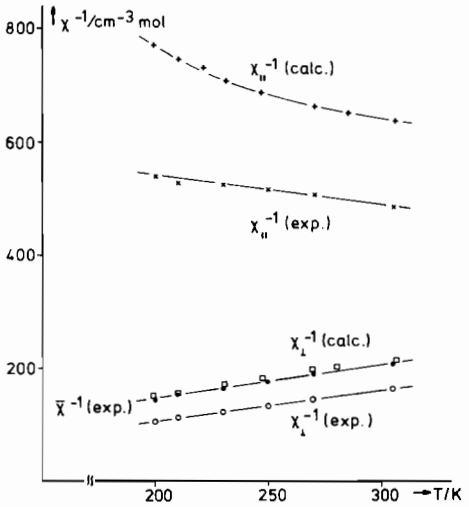

Fig. 3. χ^{-1}-*vs*-T plots of χ(exp.) and χ(calc.) of $[NBu_4^n][Cp_3PrNCBH_3]$. χ(exp.)-values based on solid straight line of Fig. 2 and $\bar{\chi}$ of $Cp_3Pr(CH_3COOCH_3)$. $\bar{\chi}$(calc.)-plot almost coincides with $\bar{\chi}$(exp.)-plot and has been omitted.

The question arises whether the inequality: $(\chi_{\parallel} - \chi_{\perp})_{calc.} < (\chi_{\parallel} - \chi_{\perp})_{exp.}$ is mainly due to (minor) deficiencies in the assessment of the NMR-data and/or to any ambiguity regarding the choice of basic parameters for the computational fitting procedure. In particular, it is not unlikely that the commonly used McConnell dipolar expression of the geometry factor [17, 24] might not account sufficiently for the influence of non-negligible spin density transfer from the metal ion onto more closely bonded ligand atoms. Likewise, it is hard to make sure that in the rapid equilibrium

$$[Cp_3Pr]_n + nL \overset{CD_2Cl_2}{\rightleftharpoons} nCp_3PrL \; (n = 1 \text{ or } > 1; \; L = CH_3CN \text{ or } BH_3CN^-) \quad (5)$$

the 1:1 adduct predominates when Cp_3Pr and L are present in equimolar amounts; base-free Cp_3Pr is, after all, also surprisingly soluble in CH_2Cl_2 [25]. Furthermore, when $L = NCBH_3^-$, the adduct $[(Cp_3Pr)_2L]^-$ is also known to exist (see next section).

Despite some minor deficiencies, however, the similarities of the corresponding χ(exp.)- and χ(calc.)-plots of Fig. 3 are satisfactory enough to state that the CF-splitting pattern independently deduced by Amberger and Edelstein is principally in good accordance with the NMR spectroscopic assessment. Importantly, the class of adducts Cp_3PrL is not tractable in terms of the frequently- quoted high-temperature approximation of Δ^{dip} introduced by Bleaney [26] in 1972 (eqn. 6)

$$\Delta_i^{dip} = G_i \cdot \frac{g_J^2 \cdot \beta^2}{60(kT)^2} \cdot 2A_2^0\langle r^2\rangle J(J+1)(2J+3)\langle J||\alpha||J\rangle \quad (6)$$

This states that if all CF-states originating from the lowest J-manifold of the Ln^{n+}-ion are thermally equally populated, Δ^{dip} is proportional only to the second-order crystal field splitting parameter, $A_2^0\langle r^2\rangle$, the reciprocal square of the absolute temperature, T^{-2}, and a Ln^{n+}-specific, tabulated [26(a)] 'Bleaney-factor', $g_J^2J(J+1)(2J-1)(2J+3)\langle J||\alpha||J\rangle$. For the Cp_3PrL-systems investigated, Δ^{dip} is neither proportional to T^{-2} between T = 200 to 300 K, nor does the (positive!) value [28] of $A_2^0\langle r^2\rangle = B_2^0$ deduced *e.g.* for T = 300 K from eqn. 6 accord with the B_2^0-value resulting from the combined MCD- and NIR/VIS-spectroscopic analysis [23] (Table III). It may be recalled, however, that an early point-charge treatment of Cp_3Ln-systems of the assumed CF-symmetry C_{3h} has led to $B_2^0 = -264$ cm^{-1} [51(a)], while from an attempted fit of the bulk magnetic susceptibility of the complex $Cp_3YbCNC_6H_{11}$ a value of -280 cm^{-1} appeared most promising [51(b)].

It is seen from Table IV that the Δ^{dip}-values of the two homologous $[Cp_3LnNCBH_3]^-$ systems with Ln = Pr and Nd are rather similar. Although this similarity might be inferred from the corresponding 'Bleaney-factors', both the NMR-derived $\chi_{\parallel}$- and $\chi_{\perp}$-values again agree very satisfactorily with the corresponding MCD- and NIR/VIS-derived quantities.

While apparently various homologous series of Ln-complexes that fulfill Bleaney's rule (eqn. 6) are known [29], the complexes Cp_3LnL seem to belong to the rare examples in which the total CF-splitting

TABLE III. Comparison of $B_2^0 = A_2^0\langle r^2\rangle$-values (in cm^{-1}) of Cp_3LnL Deduced by Different Methods.

T/K	B_2^0/cm^{-1} Cp_3PrL	B_2^0/cm^{-1} Cp_3NdL	Remarks
305	−413	−576	this work, calculation based
250	−381	−526	on eqn. 6; $L = NCBH_3^-$
200	−331	−450	
300	166–234	247–370	$L = CNC_6H_{11}$ (from ref. 28)
–	−679 ($L = CNC_6H_{11}$)	−905 (L = 2-Me·THF)	from ref. 23

TABLE IV. Comparison of $\chi_{\parallel} - \chi_{\perp}$ at Variable Temperature of Cp_3PrL and Cp_3NdL.

T/K	$(\chi_{\parallel} - \chi_{\perp})^a$	$(\chi_{\parallel} - \chi_{\perp})^b$	$(\chi_{\parallel} - \chi_{\perp})^d$	$\bar{\chi}^c$	$\chi_{\parallel}$(calc.)^b	$\chi_{\perp}$(calc.)^b
305	−4955	−2699	−2585	3400	1601	4300
270	−6070	−3275	−3028	3570	1386	4662
250	−6814	−3667	−3362	3800	1355	5022
230	−7681	−4140	−3752	4775	1315	5455
210	−8651	−4594	−4212	4400	1337	5931
200	−9250	−4903	−4530	4620	1351	6254

[a] Ln = Pr (from NMR, see Fig. 3). [b] Ln = Nd (from NMR). [c] Ln = Nd (exper. data, from ref. [51(b)]). [d] Ln = Nd, Calc. [22].

of their lowest J-manifolds ($^3H_4$ and $^4I_{9/2}$, respectively) exceed by $\geqslant 650$ cm^{-1} the average thermal energy kT $\hat{=}$ 210 cm^{-1} (for T = 300 K). Pioneering studies regarding the range of validity of Bleaney's rule have been presented earlier by Horrocks *et al.* for a number of non-organometallic lanthanide complexes [30], and further interesting insights are expected as our current examination of the organometallic Cp_3LnL series is expanded towards some of the heavier Ln-elements.

$[Cp_3^fML_n]^q$-systems with Anionic Ligands L; n = $\frac{1}{2}$ or 1; R = H

Quite unexpectedly, reaction of equimolar amounts of the ion pair $[NBu_4^n][Cp_3PrNCBH_3]$ and base-free Cp_3Pr in CD_2Cl_2 solution leads to the novel ion pair $[NBu_4^n][(Cp_3Pr)_2(\mu\text{-}NCBH_3)]$, as is indicated by the spectacular change of the δ-*vs*-T^{-1} plot of the BH_3-protons in Fig. 4 (transition from curve A to curve D). The linearity of curve D suggests that the equilibrium

$$[Cp_3PrNCBH_3]^- + CP_3Pr \overset{CD_2Cl_2}{\rightleftharpoons} [(Cp_3Pr)_2(\mu\text{-}NCBH_3)]^- \quad (7)$$

is, between 200 and 300 K, almost completely on the right side. The vibrational infrared spectra of the solid 2:1 adduct are in full accord with the assumption of a μ-$NCBH_3$ ligand which is N-bonded to one Cp_3Pr moiety and η^3-coordinated via three equivalent hydrides to the other (*cf.* Fig. 5). The formation of a corresponding Nd-complex must be deduced from very similar NMR-spectroscopic results, whereas more complicated spectra are found when two different Ln^{3+}-elements are involved in the formation of the binuclear species [31].

Likewise, the very pronounced high-field shifts of BH_4- and AlH_4-'protons', as monitored in the presence of Cp_3Pr (*cf.* curves B and C in Fig. 4), document that direct interaction of the corresponding hydride groups with the lanthanide ion is facile even in the presence of large amounts of the competitive Lewis base THF. In the latter two cases, however, the question of ligand exchange equilibria, as well as of potential EH_4-bridging (E = B or Al) deserves further examination.

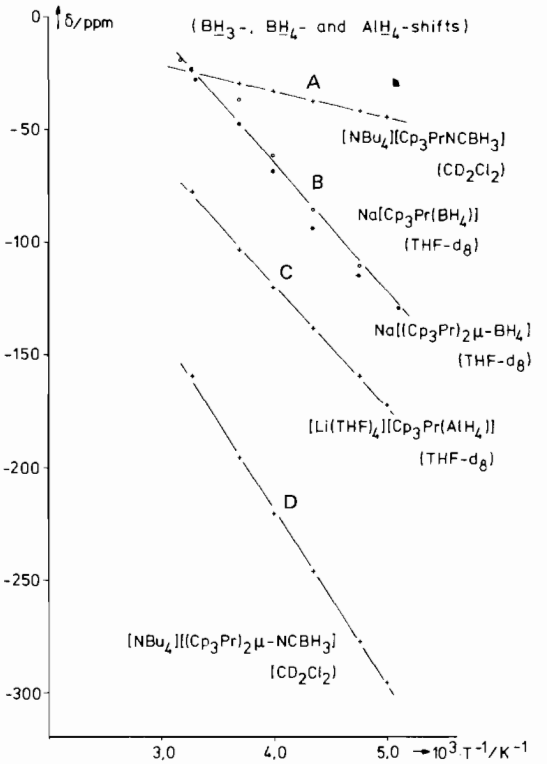

Fig. 4. δ-*vs*-T^{-1} plots of $B\underline{H}_3$-, $B\underline{H}_4$- and $Al\underline{H}_4$-hydrogen shifts of various Cp_3LnL- and $[(Cp_3Ln)_2(\mu\text{-}L)]$-species with Ln = Pr. All spectra show the relative intensities of the Cp-proton and hydride resonances as expected from the stoichiometry of the sample.

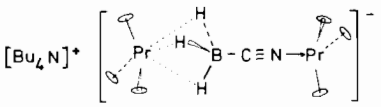

Fig. 5. Schematic description of the structure NMR-spectroscopically deduced for $[(Cp_3Ln)_2(\mu\text{-}NCBH_3)]^-$-systems.

Figure 6 presents a survey over the variation of δ of the 15 equivalent Cp ring protons of various $[Cp_3PrL_n]^q$-adducts. The linear curve A of the 1:1

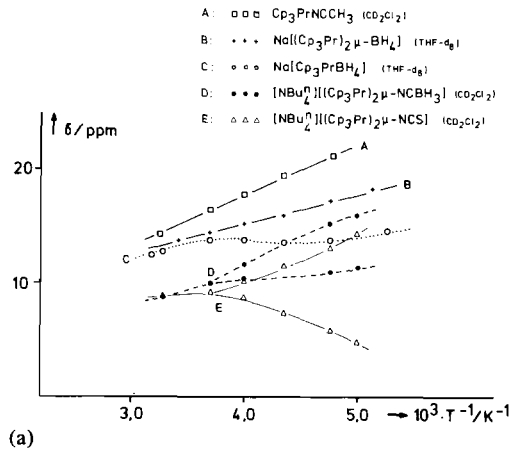

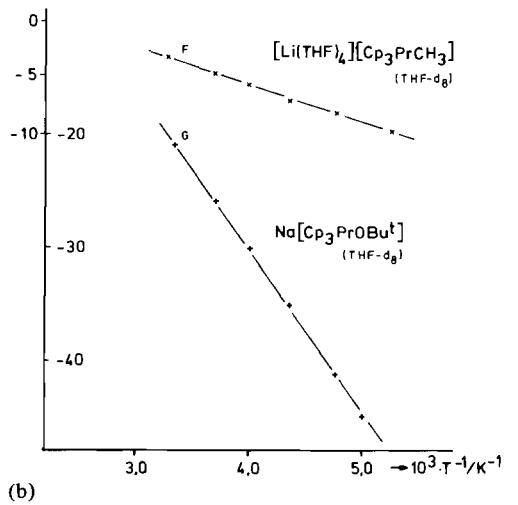

Fig. 6. δ-*vs*-T^{-1} plots of the Cp ring protons of various $[Cp_3PrL]^q$ and $[(Cp_3Pr)_2(\mu\text{-}L)]^-$-species (q = 0 or −1).

adduct with L = $NCBH_3^-$ is also representative of the majority of 1:1 adducts involving uncharged Lewis bases (*e.g.* nitriles, isocyanides, pyridines, carboxylic esters, amides etc.). Curve B and the (weakly sigmoid) curve C of Fig. 6, which correspond to THF-d_8 solutions of Cp_3Pr and $NaBH_4$ in the molar ratios 2:1 and 1:1 respectively, differ slightly by location and shape suggesting in fact the verification of bridging and non-bridging BH_4-ligands. Curve D splits below *ca.* −30 °C into two different branches, which confirms the expected non-equivalence of the two $NCBH_3$-bridged Cp_3Pr-groups. In view of the larger localization of the negative charge around the BH_3-part, the upper branch of curve D is more likely to be assigned to the N-coordinated Cp_3Pr-moiety.

According to some preliminary results, the appropriate variation of the individual Ln-ions in the bimetallic 2:1 adduct offers a wide field of new insights. Thus the $NCBH_3^-$-ligand can successfully be replaced by the related NCS^--ligand as well as by the anions CN^-, I^- and Br^- [31]. Again, a 1:1- and a 2:1-adduct may be arrived at, and detected by NMR-spectroscopy (*cf.* curves E and E′ in Fig. 6 for μ-L = NCS^-). Curve E is, like curve D, split into two low-temperature branches.

It is further revealed by Fig. 6 that the δ-value of the Cp-protons becomes less positive, and in some instances even negative, whenever L is an anion, the most striking examples being L = alkyl$^-$ and Bu^tO^-. Assuming that the value of the contact term Δ^{con} is less affected than the dipolar contribution Δ^{dip}, this gradual high-field shift of Δ^{iso} would correspond to a change of the (negative) magnetic anisotropy term $\chi_{\parallel} - \chi_{\perp}$ towards values less negative than in uncharged adducts Cp_3PrL. The feasibility of this deduction is further illustrated by comparing the Δ^{iso}-values of all H-atoms in the two adducts with L = NHR_2 and the formal n-C_4H_9-anion at two different temperatures (Table V). Anticipating negligible Δ^{con}-contributions and positive geometric factors for all H-atoms in the β-, γ-, and δ-positions, then the sign inversion of Δ_β^{dip} and Δ_γ^{dip} respectively indicates that the initially negative value of $(\chi_{\parallel} - \chi_{\perp})$ (for L = $NHEt_2$) should become weakly positive for L = n-$C_4H_9^-$.

While representative $(\chi_{\parallel} - \chi_{\perp})$ values of the two sub-classes with X = (η^1-) alkyl, vinyl or aryl on one hand, and X = η^3-H_3BR (R = H, alkyl, aryl) on the

TABLE V. Comparison of Δ^{iso}-values of Different H-atoms in the Adducts $Cp_3Pr{\cdot}NHR_2$ and $[Cp_3Pr(n\text{-}C_4H_9)]^-$.

Ligand	Temp.	Cp	α-H	β-H	γ-H[a]	δ-H[a]
$NHEt_2$	309 K	−7.0	46.4	27.8	14.2	–
	230 K	−12.1	[c]	67.2[b]	35.8	–
				73.7[b]		
$NH(Bu_2^n)$	307 K	−7.1	[c]	24.2	13.8	6.8
Bu^n	304 K	10.0	8.6	−10.41	−3.0	−0.7
	241 K	11.0	10.0	−15.41	−5.4	−1.0

[a] $\Delta^{iso} \approx \Delta^{dip}$. [b] Diastereotopic $\underline{CH_2}$ group. [c] Not detectable.

TABLE VI. Variation of $\chi_{\parallel} - \chi_{\perp}$, $\bar{\chi}$, $\chi_{\parallel}$ and $\chi_{\perp}$ (All Units of $cm^3\ mol^{-1}$) of Different $Cp_3U^{IV}X$-systems.

Ligand X	$(\chi_{\parallel} - \chi_{\perp})10^{-6}$	$\bar{\chi} \times 10^6$	$\chi_{\parallel} \times 10^6$	$\chi_{\perp} \times 10^6$
η^1-R[a]	−4500 to −4000	2958 [32]	−42 to 290	4458 to 4290
η^3-H_3BR[b]	−2320	2488 [66[e]]	940	3260
η^5-C_5H_5	0	2270 [67]	2270	2270
Cl[c,g]	1540	3346 [68]	4373	3859
OR[d]	*ca.* 2860	2521 [66[f]]	4728	1568
OCH_3	*ca.* 1375[h]			

[a]Calculated from optimal slope of Δ_i^{dip}-*vs*-G_i plots based on data from ref. [32]. [b]Calculated from optimal slope of Δ_i^{dip}-*vs*-G_i plot based on data from ref. [33]. [c]Calculated from $\chi_{\parallel} - \chi_{\perp}$ of Cp_3UR and $\Delta^{dip}(H\delta) = \Delta^{iso}(H\delta)$ of Cp_3UOBu^n adopting eqn. 8. [d]Cp′ = $C_5H_4CH_2C_6H_5$; recalculated from reported data assuming one singular conformer of C_3-symmetry (*i.e.* non-rotating Cp′-ligands, cf. ref. [44]). [e]R = H. [f]R = C_2H_5. [g]For X = F, $\chi_{\parallel} - \chi_{\perp}$ has also been shown to be positive [72]. [h]Derived from $\Delta^{con}(OCH_3) \approx -28$ ppm as estimated by INDO-calculations [33].

TABLE VII. Comparison of the Δ^{iso}-values of $Cp_3U(n\text{-}C_4H_9)$ and $Cp_3UO(n\text{-}C_4H_9)$.

	Cp	$CH_2(\alpha)$	$CH_2(\beta)$	$CH_2(\gamma)$	$CH_n(\delta)$[a]
Δ_1^{iso} (X = OBu^n)	23.93	–	−54.12	−15.59	−7.91
Δ_2^{iso} (X = Bu^n)	9.03	194.12	27.72	21.72	12.82
$\Delta_1^{iso}/\Delta_2^{iso}$	2.65	–	−1.95	−0.72	−0.62
$\Delta_1^{iso}(\delta)/\Delta_1^{iso}(\gamma)$[b]			0.287	0.51	
$\Delta_2^{iso}(\delta)/\Delta_2^{iso}(\gamma)$[b]			0.783	0.59	

[a]n = 2 or 3; [b]and of $\Delta_i^{iso}(\gamma)/\Delta_i^{iso}(\beta)$, respectively.

other, have been derived from the slopes of the corresponding optimal Δ_i^{dip}-*vs*-G_i plots based on extensive calculations of Δ^{dip} and Δ^{con} from Δ^{iso} [32, 33], a first estimate of $\chi_{\parallel} - \chi_{\perp}$ of the complex $Cp_3UO(n\text{-}C_4H_9)$ is based on the applicability of eqn. 8.

$$\frac{\Delta_i^{dip}(X)}{\Delta_i^{dip}(X')} = \frac{\Delta_j^{dip}(X)}{\Delta_j^{dip}(X')} = \frac{(\chi_{\parallel} - \chi_{\perp})_x}{(\chi_{\parallel} - \chi_{\perp})_{x'}} \quad (T = \text{const.}) \quad (8)$$

Assuming that the two pairs of methylene protons of the γ- and δ-C-atoms of X = n-C_4H_9 and X′ = O(n-C_4H_9) respectively have identical geometry factors (*i.e.* $G_\gamma(X) \approx G_\gamma(X')$ and $G_\delta(X) \approx G_\delta(X')$), then $(\chi_{\parallel} - \chi_{\perp})_{x'}$ may be obtained from ratio $\Delta_\delta^{dip}(X)/\Delta_\delta^{dip}(X')$ and $(\chi_{\parallel} - \chi_{\perp})_x$. The data in the two lowest lines of Table VII show that the bordering conditions justifying this procedure are approximately met. The same does not hold for corresponding pairs of complexes involving the anionic systems $[Cp_3Pr(n\text{-}C_4H_9)]^-$ and $[Cp_3U^{III}(n\text{-}C_4H_9)]^-$ [34] where complications owing to the presence of counter-cations are not unlikely.

Another unexpected phenomenon displayed by the paramagnetic salts, or ion-pairs, $[NBu_4^n][(Cp_3Pr)_nX]$ (n = 1 or 2) is that the proton resonances of the organic counter-cation $[NBu_4^n]^+$ of the anionic adducts also show surprisingly large isotropic shifts (Fig. 7). Again the observed $|\Delta^{iso}|$-values increase with decreasing temperature and are comparable in magnitude with the corresponding shifts of some dissolved salts $[(NBu_4^n)_2][^dMX_4]$ involving paramagnetic d-transition metals (Ni^{2+}, Co^{2+} etc., X =

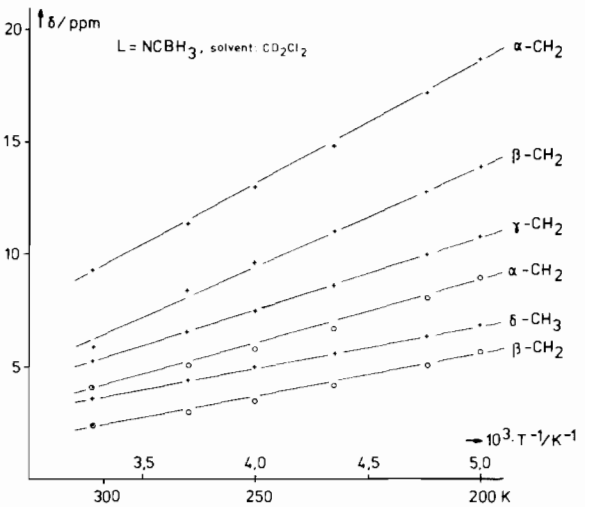

Fig. 7. δ-*vs*-T^{-1} plots of Bu^n-protons of the ion pairs $[NBu_4^n][Cp_3PrL]$ (○○○) and $[NBu_4^n][(Cp_3Pr)_2(\mu\text{-}L)]$ (+++).

halide ions [35]). On the other hand, paramagnetic organo-uranium salts of the general type $[NBu_4^n]$-$[Cp_3U^{IV}XY]$ (X and/or Y = NCS, $NCBH_3$, OCN etc.; see section 6) are devoid of noticeable isotropic shifts of the alkyl proton resonances. While the reason for the paramagnetic shifting of the alkyl resonances in the presence of anionic organo-lanthanoid adducts is not yet clear, this effect serves as a useful indicator of the chemical interaction of Cp_3Ln-molecules with a variety of anionic Lewis bases L^- that cannot themselves be subjected to NMR experiments.

$Cp_3{}^fML_n$-systems with n = 0 (Cp = C_5H_4R)

It would be likewise of interest to analyze the NMR-spectroscopic behaviour and the underlying electronic structure of Cp_3Ln-complexes devoid of any additional ligand L, but in particular the corresponding complexes of the lighter lanthanoids are too insoluble in non-coordinating solvents to solve this question experimentally. From the results of a recent X-ray crystallographic study of the complex Cp_3Pr [36] it may be deduced that the mononuclear complexes involving the rather large cations La^{3+}–Nd^{3+} are noticeably undercoordinated [37] and show a pronounced tendency to associate to highly insoluble oligomers in the absence of coordinatively sufficiently active molecules. Even the complex $(CH_3C_5H_4)_3Nd$ (=$(MeCp)_3Nd$) is known to form MeCp-bridged tetramers in the solid state [38]; however, the complexes $(MeCp)_3Ln$, even of the lighter Ln-elements, are sufficiently soluble for NMR-studies *e.g.* in toluene.

Like most of the known $(MeCp)_3{}^fML$-systems, the L-free Ln-complexes also give rise to two usually widely spaced C_5H_4R-ring hydrogen resonances, (*vide infra*). Figure 8 shows that between at least −70 and +30 °C the δ-*vs*-T^{-1} plots of both $(MeCp)_3Yb$ and the adduct $(MeCp)_3Yb{\cdot}CNCMe_3$ are straight lines. The same is also true for the adduct $(MeCp)_3Pr{\cdot}CNCMe_3$, while the L-free Pr-complex displays a completely different NMR-behaviour (Fig. 9). Only around room temperature are three distinct singlets of the expected relative intensities 2:2:3 apparent. Between *ca.* −10 and −50 °C each of these resonances passes, after considerable broadening, an individual coalescence temperature, and at about −70 °C a total of seven new resonances emerges within a surprisingly wide range of almost 250 ppm. Evidently, some of the ring hydrogen atoms show at −70 °C resonances at rather remote high-field positions, while *e.g.* at room temperature all C_5H_4-resonances appear in low-field positions relative to the diamagnetic standard $(MeCp)_3La$. The unusual shapes of the two δ-*vs*-T^{-1} plots (a) and (b) of Fig. 9 below *ca.* 35 °C deviate strongly from the usual proportionality of $|\delta|$ and

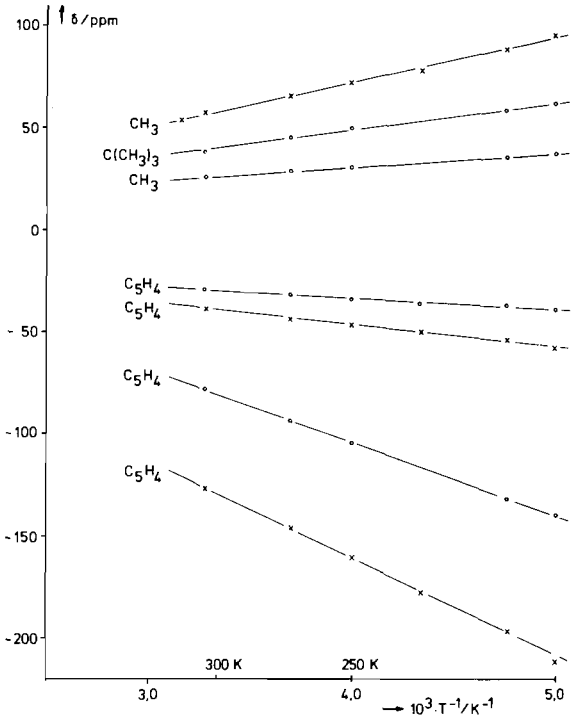

Fig. 8. δ-*vs*-T^{-1} plots of different H-atoms of the complexes $(C_5H_4CH_3)_3Yb$ (X X X) and $(C_5H_4CH_3)_3YbCNCMe_3$ (O O O) (solvent: toluene-d_8).

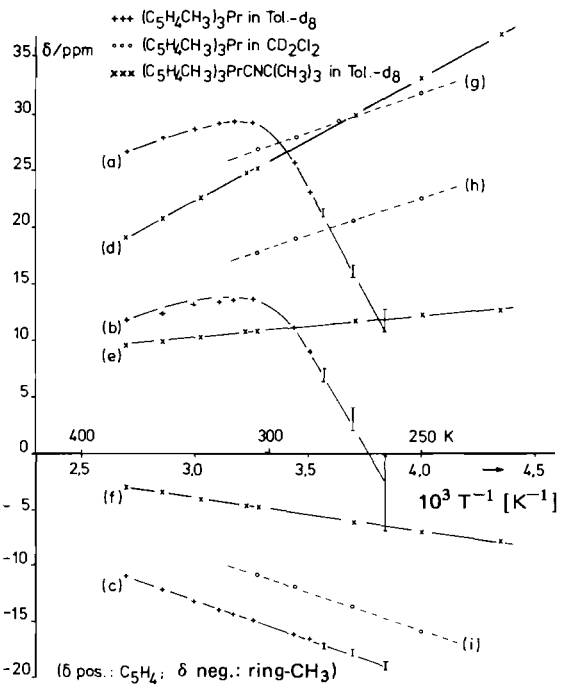

Fig. 9. Comparison of δ-*vs*-T^{-1} plots of H-atoms bonded in $(C_5H_4CH_3)_3Pr$ dissolved in toluene-d_8, CD_2Cl_2 and CD_3CN, respectively, and $(C_5H_4CH_3)_3PrCNCMe_3$ (in toluene-d_8). Vertical bars indicate increasing line broadening.

T^{-1} reflect the continuous high-field shift of the (average) ring proton resonances as the temperature is decreased.

Independently performed studies of the temperature dependence of the paramagnetic susceptibility $\bar{\chi}$ of $(MeCp)_3Pr$-solutions in toluene following Evans' method [11] did not reveal any significant deviation from the Curie–Weiss law; on the other hand, cryoscopic molecular weight studies in benzene solution indicate unambiguously that $(MeCp)_3Pr$ is, unlike $(MeCp)_3Yb$, partially associated [39]. Assuming, like for crystalline $[(MeCp_3Nd]_4$, a preferential tetramer of the Pr-homologue in solution, the cryoscopic result would point out that at *ca.* +5 °C about 25% of all $(MeCp)_3Pr$-units would be components of the tetramer $[(MeCp)_3Pr]_4$. Hence, the ^1H NMR spectra above the coalescence points reflect only the average resonances of the very rapidly interconverting monomers and oligomers of eqn. 9:

$$n(MeCp)_3Pr \underset{\text{very rapid}}{\overset{C_6H_6 \text{ or } C_6H_5Me}{\rightleftharpoons}} [(MeCp)_3Pr]_n + [(MeCp)_3Pr]_m + \ldots \quad (9)$$

The pronounced high-field shift in the low-temperature (−70 °C) spectra is probably due to those ring H-atoms of μ-MeCp ligands which lie closest to the metal ion of the next $(MeCp)_3Pr$-unit (Fig. 11). It can

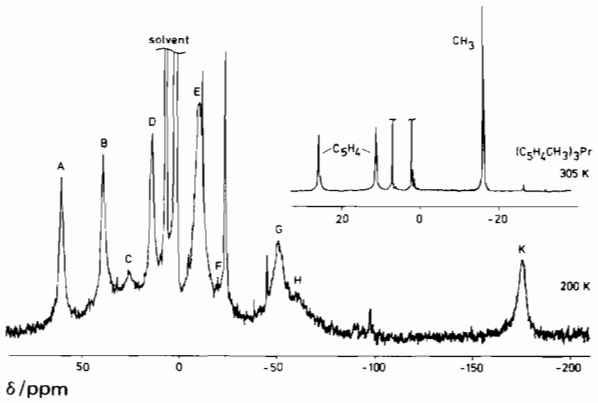

Fig. 10. ^1H NMR spectra of $[(C_5H_4CH_3)_3Pr]_n$ at 305 and 200 K.

be shown that relative to the trigonal rotational main axis of the latter moiety the geometry factors of such μ-ring H-atoms adopt rather large positive values. In view of the usually negative paramagnetic anisotropy, $\chi_{\parallel} - \chi_{\perp}$, of Cp_3PrL-systems (*vide supra*), at least one H-atom of a bridging MeCp-ligand should in fact give rise to a pronounced high-field shift.

As the steric bulk of the ring substituent R of a complex $(C_5H_4R)_3Ln$ (Ln = La–Nd) is increased further, the solubility in non-coordinating solvents increases, and the tendency to oligomerize is strongly reduced. Thus, the complex $(C_5H_4SiMe_3)_3Pr$ is a monomer in benzene solution, its toluene-d_8 solution giving rise to a δ-*vs*-T^{-1} diagram that consists of three nearly straight lines between +30 and −70 °C (Fig. 12). Both the very wide separation of the two ring-

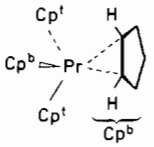

Fig. 11. Schematic description of one Cp_3Pr-moiety interacting with a bridging Cp ligand of another Cp_3Pr complex *via* one or two Cp-ring C-atoms.

H resonances (relative intensity: 2) relative to the corresponding separation found for various $(MeCp)_3PrL$-systems (*cf.* Fig. 9) and the surprisingly large high-field shift of the $SiMe_3$-singlet (relative intensity: 9) as compared with the position of the CH_3-resonances of $(MeCp)_3PrL$-systems suggest that the three bulky $SiMe_3$-groups force each of the three ring ligands into one favourite conformation, most plausibly the only one that strictly retains trigonal symmetry (compare Fig. 13).

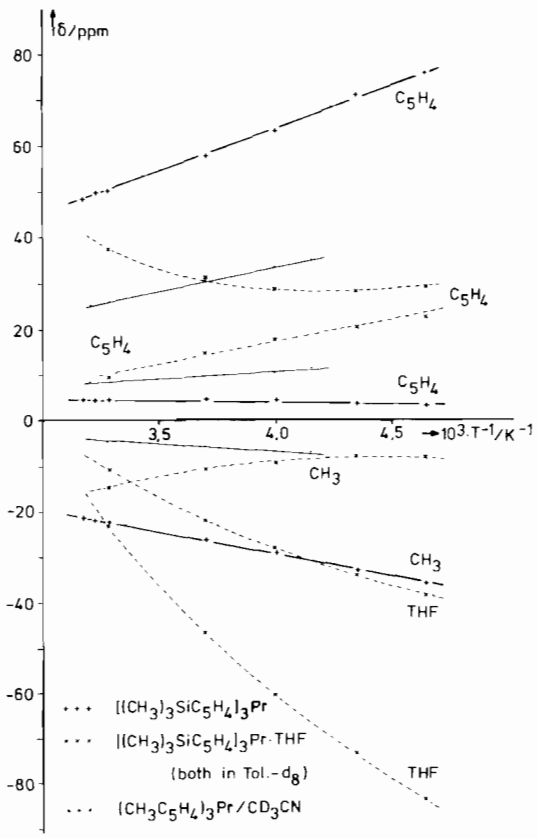

Fig. 12. δ-*vs*-T^{-1} diagrams of $(C_5H_4SiMe_3)_3Pr$ and $(C_5H_4SiMe_3)_3Pr \cdot THF$ in toluene-d_8 and $(C_5H_4CH_3)_3Pr$ in CD_3CN ($\hat{=}$ $(C_5H_4CH_3)_3PrNCCD_3$).

This suggestion is supported by the unusual appearance of the δ-*vs*-T^{-1} plots of all proton resonances of the adduct $(C_5H_4SiMe_3)_3Pr_3 \cdot THF$ (dotted curves in Fig. 12). None of these plots is strictly linear, the two C_5H_4-plots tend to converge rather than to diverge at very low temperatures, and one of them even displays a smooth minimum at *ca.* −20 °C. Most probably, the three large $SiMe_3$-groups not only freeze in the otherwise very rapid rotation of the C_5H_4R-ligands about their pseudo-five fold axes, but also inhibit the occupation of the empty axial position by an extra ligand L.

As the chemical shift δ of the $SiMe_3$-protons approximately equals the corresponding dipolar shift Δ^{dip}, the temperature dependence of the quantity $\chi_{\parallel} - \chi_{\perp}$ of base-free $(C_5H_4SiMe_3)_3Pr$ could in principle be estimated by adopting a realistic average value of the geometry factor of the nine equivalent $SiMe_3$ H-atoms. By subtracting the likewise calculable Δ^{dip}-values of the two non-equivalent C_5H_4 H-atoms (in the α- and β-positions relative to the $SiMe_3$-group) from the two observed Δ^{iso}-values, two alternative pairs of Δ^{con}-values for the α- and β-H atoms are obtained. Most interestingly, either of the two (hypothetical) alternative pairs of $\Delta_\alpha{}^{con}$ and $\Delta_\beta{}^{con}$ that are obtained in this way consists of values of opposite sign; this feature is very reminiscent of results of very simple deductions of $\Delta_\alpha{}^{con}$ and $\Delta_\beta{}^{con}$ for $(C_5H_4R)_3$-UX- and $(C_5H_4R)_2UX_2$-complexes (*vide infra*). Assuming, on the other hand, freely rotating MeCp-ligands in the case of all known $(MeCp)_3PrL$-systems, and the same $(\chi_{\parallel} - \chi_{\perp})$-values as have been evaluated for the corresponding Cp_3PrL homologues (*cf.* Section 1), one of the two calculated Δ^{con}-values likewise becomes more positive than for the simpler homologue, while the other adopts a temperature-independent value close to zero.

Figure 8 shows for comparison the temperature dependence of all different types of H-atoms present in the complexes Cp_3Yb, $(MeCp)_3Yb$ and $(MeCp)_3$-$YbCNCMe_3$ respectively. It is seen that the three MeCp-resonances of the latter two complexes give rise to non-superimposable δ-*vs*-T^{-1} plots. In view of the noticeably smaller ionic radius of Yb^{3+} as compared with Pr^{3+}, this difference might also be explained in terms of non-rotating MeCp-ligands. Alternatively, by the absence of the Lewis base ligand, considerable changes of the electronic structure might be caused. Another interesting observation is that at temperatures below −30 °C the ring methyl resonance of the complex $(MeCp)_3PrCNC_6H_{11}$ is split into two components (200 K: δ_1 = 41.6 ppm, δ_2 = 44.3 ppm; intensity ratio 2:1) whereas any distinct resonances of the conformer involving an axially substituted cyclohexyl group are missing [40]. Primarily this result indicates that at low temperatures free rotation about the practically linear $Pr{-}C{\equiv}N{-}C(H\alpha)C_5H_{10}$ axis (but not necessarily about the three C_5H_4Me ring normals) is no longer possible (Figs. 13, 14).

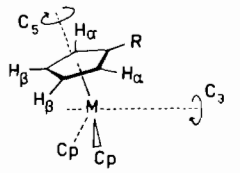

Ring Proton(s)	H_α	H_β	$\bar{H}_{(rotating\ ring)}$
$G(\nu, R)/cm^{-3}$	-32,764	+10,480	$-9{,}463 \cdot 10^{21}$

Fig. 13. Schematic view on one substituted (and assumedly non-rotating) Cp-ligand of $(C_5H_4R)_3Pr$ with pyramidal ring normals (above), and comparison of geometry factors G_i of Cp-ring H-atoms under different conditions (below).

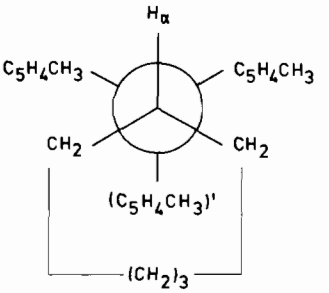

Fig. 14. Newman-projection of the complex $(C_5H_4CH_3)_3$-$YbCNC_6H_{11}$, viewed along its Yb–C≡N–C-axis.

Influence of R on $(\eta^n\text{-}C_nH_{n-1}R)_m{}^fMX_k$-systems (n = 8 or 5; k = 0, 1, 2)

According to the above interpretation of the NMR-spectrum of the complex $(C_5H_4SiMe_3)_3Pr$, introduction of one $SiMe_3$ group into each C_5H_5-ring apparently makes the free spin densities on the four remaining (pairwise equal) H-atoms increase and decrease respectively, relative to the value of the unsubstituted C_5H_5-ligand. This phenomenon appears to be quite independent of the size of the coordinated C_nH_{n-1} R-ligand and of the nature of the paramagnetic central metal ion. Thus Streitwieser *et al.* [8] have pointed out that the observed isotropic ^1H NMR shifts of the ring H-atoms of 1,1′-disubstituted uranocenes, $(\eta^8\text{-}C_8H_7R)_2U$, R = *e.g.* alkyl, aryl, alkoxide), no longer give rise to one singlet, but to four singlets (relative intensites 2:2:2:1) whose centre of gravity coincides practically with the resonance of unsubstituted uranocene. Figure 15 illustrates that the same also holds for various 1,1′-disilylated uranocenes [41]. As all ring H-atoms of the substituted sandwich complexes should experience the same dipolar shifts, the splitting of the unique ring proton singlet of $(C_8H_8)_2U$ should, after ring substitution, immediately reflect the resulting modifications of the contact contributions, $\Delta_i{}^{con}$.

The same statement would apply to various $(C_5H_4R)_nU^{IV}X_{4-n}$-systems (n = 2 or 3; X = a most probably η^3-coordinated [42] BH_4-ligand), however in such cases it is more difficult to decide whether the

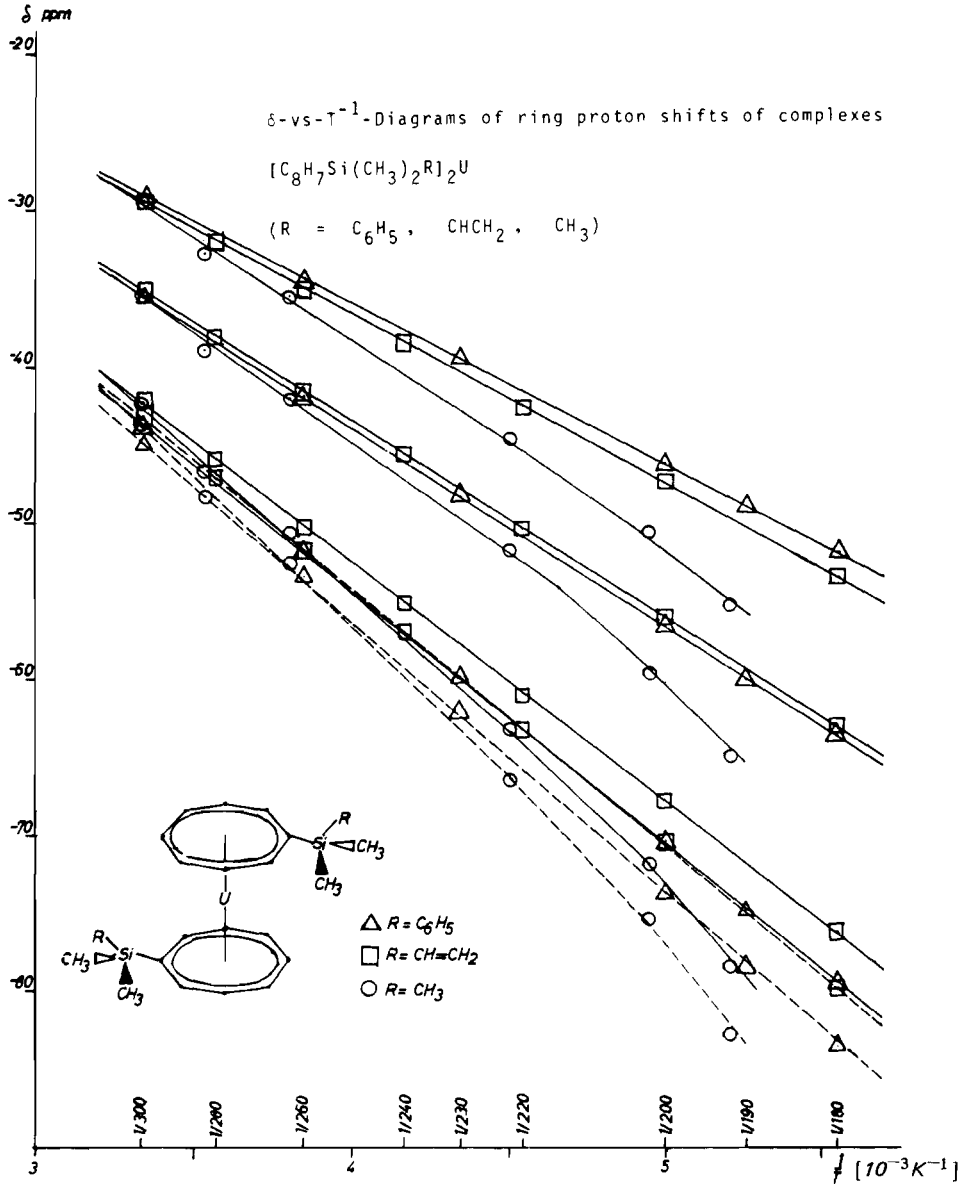

Fig. 15. δ-*vs*-T^{-1} diagrams of three uranocene derivatives $[(CH_3)_2RSiC_8H_7]_2U$ (solvent: toluene-d_8) [41]).

particular shape of R will prevent the cyclic ligand from rapid rotation [13] or not. According to simple steric considerations, free rotation should undoubtedly be allowed in the species with n = 2. Hence, the rather large separations of isothermal points on the two pairs of curves 1,1′ and 3,3′, respectively (Fig. 16), will equal directly the difference $|\Delta_\alpha^{con} - \Delta_\beta^{con}|$.

Quite surprisingly, rather similar δ-*vs*-T^{-1} plots result from the high-field and low-field resonances of the two corresponding complexes with n = 3 (curves 2,2′ and 4,4′, respectively, of Fig. 16). As it also appears justified to assume freely-rotating ring ligands for the complex $(MeCp)_3UNCBH_3$, the rather unchanged NMR-features observed for its $SiMe_3$-substituted homologue favour the suggestion that even three η^5-$C_5H_4SiMe_3$-ligands may rotate rapidly about their ring centre-to-U(IV) normals. Corresponding conclusions result also from the reported room temperature C_5H_4R-proton shifts of complexes of the composition $(C_5H_5)_2(C_5H_4R)UCl$ and (C_5H_5)-$(C_5H_4R)_2UCl$, respectively [43]. Recalling that the ionic radius of U(IV) is somewhat smaller than that of Pr(III), one might expect a U-bonded C_5H_4R-ligand (with large R) to rotate less freely than a corresponding Pr-bonded C_5H_4R-ring.

Table VIII presents the results of a model calculation of the ring proton Δ_i^{con}-values of the complex $(C_5H_4SiMe_3)_3UNCBH_3$ in case of freely rotating and fixed $C_5H_4SiMe_3$ ring ligands, respectively. It seems

TABLE VIII. Comparison of $\bar{\mu}_{eff}$, $\Delta^{iso}(B\underline{H}_3)$ and the Individual $\chi_{\parallel}$ and $\chi_{\perp}$-values of Three Different $[Cp_3^fM(NCBH_3)_n]^q$-systems ($G(B\underline{H}_3) = 1.019 \cdot 10^{22}$ cm^{-3}).

Compound	T/K	μ_{eff}/B.M.	$\Delta^{iso}(B\underline{H}_3)$ (ppm)	$\chi_{\parallel} \times 10^3$ (cm^3 mol^{-1})	$\chi_{\perp} \times 10^3$ (cm^3 mol^{-1})
$[NBu_4^n][(C_5H_5)_3U(NCBH_3)_2]$	305	1.87	25.0	−1.60	2.84
	200	1.57	33.9	−2.48	3.54
$(CH_3C_5H_4)_3U(NCBH_3)$	307	2.42	49.6	−2.84	5.95
	200	2.12	73.2	−4.66	8.31
$[NBu_4^n][(C_5H_5)_3Pr(NCBH_3)]$	305	3.39	24.0	2.06	6.10
	200	3.31	44.0	1.85	9.40

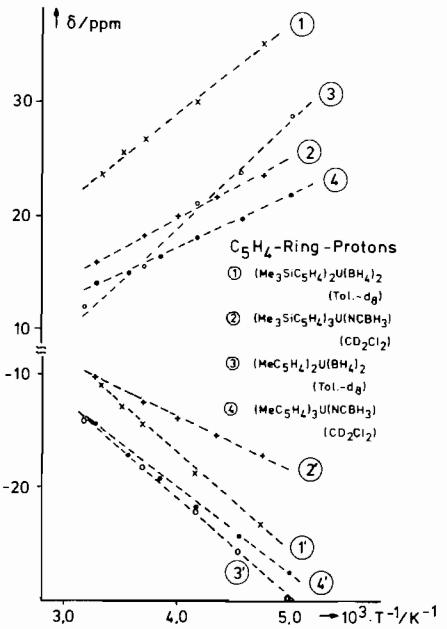

Fig. 16. Comparison of δ-*vs*-T^{-1} diagrams of two complexes $(C_5H_4R)_2U(BH_4)_2$ (curves 1 + 1′ and 2 + 2′) and $(C_5H_4R)_3U(BH_4)$, respectively (curves 3 + 3′ and 4 + 4′).

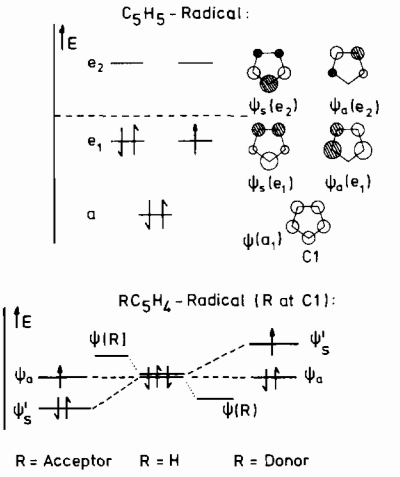

Fig. 17. Schematic description of π-HMO's of five-fold symmetric C_5H_5-radical (above) and of a symmetry-perturbed C_5H_4R-radical involving different π-interaction between R and Cl (below).

that under the latter assumption unexpectedly large deviations of Δ_{α}^{con} and Δ_{β}^{con} from the more realistic Δ^{con}-value of freely rotating ligands would result. For this reason, some recent deductions of the values of $\chi_{\parallel} - \chi_{\perp}$ and of the super-hyperfine coupling parameter of the ring H-atoms of some $(C_5H_4R)_3UCl$-systems involving substituents R like $CH_2C_6H_5$ and $SiMe_3$ under the assumption of non-rotating ring ligands [44] should be considered critically.

The commonly observed splitting of the Δ^{con}-value of freely rotating C_5H_5-ligands (which is usually positive for f^1 to f^3-systems) into one larger and one smaller $\Delta_{1,2}^{con}$-value after substitution of one ring H-atom by a group R may (in an admittedly naive manner) be rationalized by Fig. 17. Each C_5H_5- and C_5H_4R-ligand, respectively, although coordinated to a paramagnetic f^q-ion, is considered as a fictitious radical that, unlike the corresponding free radicals, accommodates only a fraction of a free electron. As long as for each ring ligand five-fold rotational symmetry is conserved, the two π-HMO's $\psi_s(e_1)$ and $\psi_a(e_1)$ (as well as $\psi_s(e_2)$ and $\psi_a(e_2)$) are equally occupied by this fraction of an electron, which corresponds to an equal distribution of its spin fraction over all five ring C-atoms. Provided that the substituent R can interact with a ring-C p_z-AO, this interaction is only possible with one component of the formerly degenerate π-HMO pair (*i.e.* with $\psi_s(e_1)$ and $\psi_s(e_2)$, respectively) which circumstance causes that, finally, ψ_a and ψ_s' are no longer degenerate. Hence, in terms of a Boltzmann population, the two orbitals ψ_a and ψ_s, and consequently the individual ring-C p_z-AO's in α- and β-position relative to R, are no longer expected to display the same free spin density. This admittedly oversimplified model however does not account for the frequently observed spin reversal for one kind of ring H-atoms (leading to opposite signs of Δ_{α}^{con} and Δ_{β}^{con}), pointing out that any more

realistic theoretical treatments would *inter alia* deserve MO-calculations on the basis of explicitly considered exchange interaction terms.

$Cp_3'^fML_n$-systems with n = 2

$Cp_3'^fM$-derivatives involving a sufficiently large central metal ion can alternatively accommodate one or two additional, preferentially rod-shaped ligand(s) L. A maximum of examples have so far been characterized with ^fM = U(IV), the general type of complex $[Cp_3UXY]^q$ being established X-ray-crystallographically for the electric charges q = 0, +1 and −1 [45–47]. In all three cases (Cp = C_5H_5), at least in the solid state, a trigonal bipyramidal coordination is realized, the ligands X and Y occupying the two (*trans*-) axial positions and the three Cp ring normals pointing towards the three (trigonal planar) equatorial positions. According to convincing analytical and (NIR/VIS-) spectroscopic data, a corresponding composition also seems possible with Np(IV) and, somewhat less readily, with Pu(IV) as the central ions [48]. $Cp_3'^fML_2$-systems with Cp' = C_5H_4R (^fM = U) have so far been observed only in solution, but, remarkably, even the complex $(C_5H_4SiMe_3)_3UNCBH_3$ seems to add one NCS^- anion [49].

Lanthanoid complexes $Cp_3'Ln^{III}L$ with Ln = Pr or any Ln(III)-ion of a higher atomic charge do not add a second ligand L', yet most recently the first two lanthanum complexes of the analytic composition $(C_5H_5)_3La(NCR)_2$ (R = CH_3 and C_2H_5) have been characterized [50]. It is worth noting that the sterically optimal conditions for the verification of trigonal bipyramidal $[Cp_3'LnXY]$-systems (*i.e.* Ln = La) have been predicted by the so-called 'solid angle sum rule' [37].

It has been suggested that the transition of a pseudotetrahedral (ψ-T_d) Cp_3UX-complex into a trigonal bipyramidal (tbp) derivative $[Cp_3UXY]^q$ is accompanied by notable changes of the f–f crystal field transitions in the NIR/VIS spectral range [48, 52] and likewise of the magnetic properties [53] (see also Table VIII). For a further elucidation of the different electronic structures of ψ-T_d- and tbp-configurated Cp_3U^{IV}-derivatives, it would appear helpful to also exploit suitable proton resonance data of H-atoms located on the axial ligand(s) X or Y. In particular, from such data the value of $\chi_\parallel - \chi_\perp$ might become accessible and, provided that $\bar{\chi}$ is known, the values of $\chi_\parallel$ and $\chi_\perp$ too. In Table VIII the calculated $\chi_\parallel$- and $\chi_\perp$-data are listed along with the experimental Δ^{iso}- and $\bar{\mu}_{eff}$-values (Δ^{iso} of $B\underline{H}_3$) of the complexes $[(C_5H_5)_3U(NCBH_3)_2]^-$, $(MeCp)_3U(NCBH_3)$ and $[(C_5H_5)_3Pr(NCBH_3)]^-$ for two different temperatures. Most unexpectedly, and unlike for the Pr-complex considered above (Section 1), $\chi_\parallel$ is negative for both uranium complexes. As $\chi_\parallel$ is proportional to a Boltzmann summation over various squared matrix elements and can never be negative, most probably one of the basic assumptions leading to the data of Table VIII cannot be valid.

It has been suggested [54] that in view of the comparatively large Δ^{iso}-values of the $NCBH_3$-H-atoms of the complexes Cp_3UNCBH_3 and $(MeCp)_3UNCBH_3$ (see Fig. 18) that these (in CD_2Cl_2-solution) ψ-T_d-shaped complexes may co-exist as two rapidly equilibrating isomers involving either an N- or

$$\underset{(A)}{Cp_3'U{\leftarrow}N{\equiv}C{-}BH_3} \overset{CH_2Cl_2}{\rightleftharpoons} \underset{(B)}{Cp_3'U(\eta^3\text{-}H_3B{-}C{\equiv}N)} \qquad (Cp' = Cp \text{ or } MeCp) \qquad (10)$$

η^3-H_3B-coordinated $NCBH_3$-ligand. Evidently, by admixture of a fraction of isomer B to A the (average) Δ_{ave}^{iso}-value of the BH_3-protons would be shifted sensibly towards higher fields, and insertion of this value into eqn. 2 furnished with the geometry factor of N-bonded $NCBH_3$ would erroneously yield a negative $\chi_\parallel$-value. In case of any direct B··H··U bonding according to (necessarily very rapid) equilibria of some isomeric tbp-varieties

$$[H_3BCN{-}\overset{\overset{\diagdown}{|}}{U}{-}NCBH_3]^- \rightleftharpoons [H_3BCN{-}\overset{\overset{\diagdown}{|}}{U}\cdot\cdot H{-}BH_2CN]^- \rightleftharpoons [NCBH_2{-}H\cdot\cdot\overset{\overset{\diagdown}{|}}{U}\cdot\cdot H{-}BH_2CN]^- \rightleftharpoons U(NCBH_3) + [NCBH_3]^- \qquad (11)$$

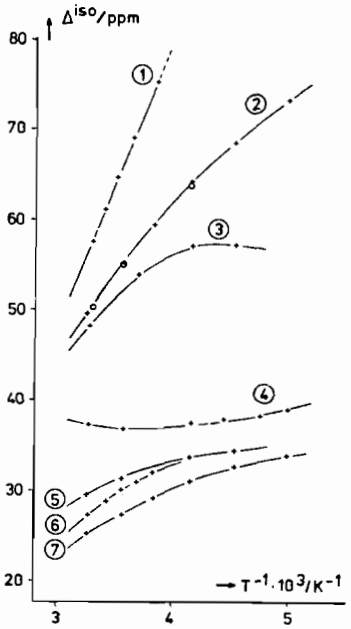

Fig. 18. Δ^{iso}-*vs*-T^{-1} diagrams of $(CH_3C_5H_4)_3U(BH_4)$ in toluene-d_8 (1), of $(CH_3C_5H_4)_3U(NCBH_3)$ in toluene-d_8 (○○○) and CD_2Cl_2 (+++) (2), THF-d_8 (5) and CD_3CN (6), of $(C_5H_5)_3U(NCBH_3)$ in CD_2Cl_2 (3), and THF-d_8 (4), and of $[(C_5H_5)_3U(NCBH_3)_2]^-$ in CD_2Cl_2 (7); from ref. [54].

TABLE IX. Comparison of Properties of Three Different Complexes of the Composition $Cp_3'U(NCBH_3)$.

Cp′	colour of complex	assumed type of coordination
C_5H_5	green	1-D-oligomer of tbp-units
$C_5H_4CH_3$	green $\underset{}{\overset{ca.\ 130\ °C}{\rightleftharpoons}}$ brown	reversible formation of oligomers and monomers
$C_5H_4SiMe_3$	brown	monomeric ψ-T_d-units

of the dissolved species $[Cp_3U(NCBH_3)_2]^-$, the rather large high-field position of the Δ^{iso}-value of its BH_3-protons (Fig. 18) could also be explained.

Direct B–H··U contacts corresponding to those assumed in eqn. 11 have been postulated for some $Cp_3'U(NCBH_3)$-complexes in the solid state [54]. The previously anticipated polymeric nature of solid $(C_5H_5)_3U(NCBH_3)$ [33] is NIR/VIS-spectroscopically in excellent accord with the assumption of $NCBH_3$-bridged $Cp_3'UXY$ of trigonal bipyramidal coordination (eqn. 12):

$$\equiv C{-}BH_2^{t}{+}H^{b}\cdots \overset{|}{\underset{|}{U}} \leftarrow N{\equiv}C{-}BH_2^{t}{+}_{n}H^{b}\cdots$$

(t: terminal; b: bridging H-atom) (12)

Table IX indicates that by increasing steric bulk of the ring-hydrogen substituent R the attractivity of the formation of zig-zag-shaped, one-dimensional oligomers composed of trigonal bipyramidal units is continuously reduced.

A non-stationary nature in solution could also be postulated for most $[Cp_3UXY]^q$-systems in view of the rather unusual curvature of the δ-*vs*-T plots of their 15 equivalent Cp-ring H-atoms (Figs. 19 and 20). Quite frequently, the curve even passes a

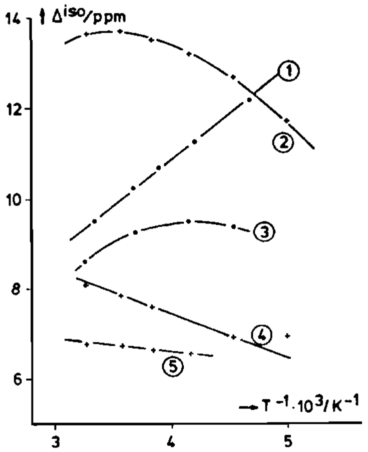

Fig. 19. Δ^{iso}-*vs*-T diagrams of the C_5H_5-protons of $(C_5H_5)_3UCl$ in CD_2Cl_2 (1), $[(C_5H_5)_3U(NCS)_2]^-$ in CD_2Cl_2 (2), $(C_5H_5)_3U(NCBH_3)$ in CD_2Cl_2 (3) and CD_3CN (5), and of $[(C_5H_5)_3U(NCBH_3)_2]^-$ in CD_2Cl_2; from ref. [54].

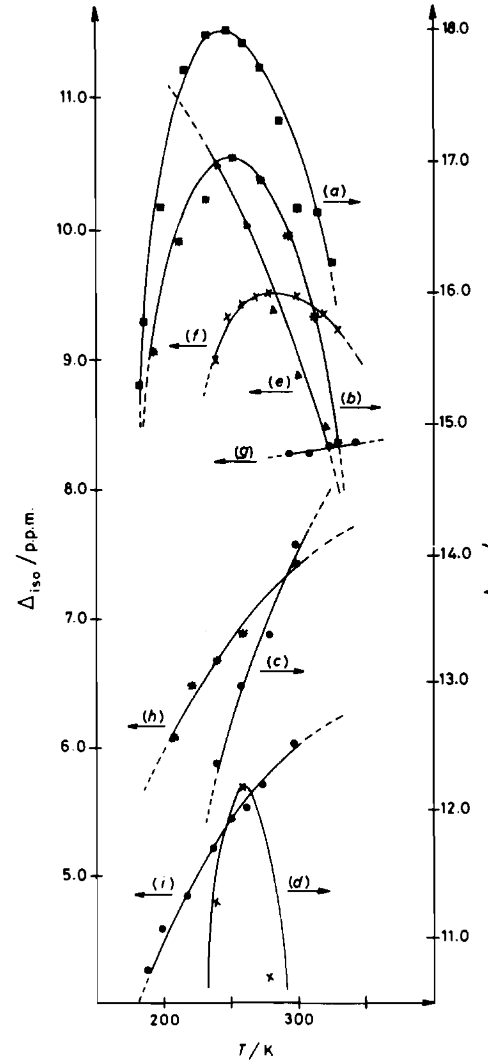

Fig. 20. Δ^{iso}-*vs*-T diagrams of $[(CH_3C_5H_4)_3U(NCS)_2]^-$ (a), $[(C_5H_5)_3U(NCS)_2]^-$ (b), $[(C_5H_5)_3U(OCN)(NCS)]^-$ (c), $[(C_5H_5)_3U(OCN)(NCMe)]$ (d), $[(C_5H_5)_3UCl(NCMe)]$ (e), $[(C_5H_5)_3U(NCS)(NCMe)]$ (f), $[(C_5H_5)_3U(H_2O)_2]^+$ (g), $[(C_5H_5)_3UC(CN)_3Cl]^-$ (h) and $[(CH_3C_5H_4)_3UC(CN)_3Cl]^-$ (i); from ref. [48].

maximum, or suggests by displaying a temperature dependence inverse to that fulfilling the familiar Curie–Weiss-law, that a maximum might eventually

be reached outside the temperature range 200 K $\leqslant$ T $\leqslant$ 310 K. The latter feature is even displayed by the cation $[(C_5H_5)_3U(H_2O)_2]^+$ assumed to be present in aqueous solutions of *e.g.* Cp_3UCl [55]. Solutions of $[Cp_3'UXY]^-$-systems involving $C_5H_4CH_3$- instead of C_5H_5- ligands give rise to very similar features for the average value Δ_{ave}^{iso} of the two expected ring proton resonances. Unlike for the corresponding ψ-T_d-systems, the two different Δ^{iso}-values are at all temperatures hardly more than 3 ppm apart from each other, suggesting that the ring H-atoms in α- and β-positions (relative to R) do not experience noticeably different contact contributions.

Ignoring here the verification of fully stationary, singular $Cp_3'UXY$-complexes of rather unusual magnetic properties, the drastic deviations from a Curie–Weiss-like, linear increase of $|\delta|$ proportional to the reciprocal temperature must be rationalized in view of very rapid intra- or inter-molecular rearrangements in solution. Primary candidates are the sterically optimal tbp-complex and its sterically less favourable isomer in which the formerly axial ligands are *cis*-, or side-on, coordinated (Fig. 21). The structurally characterized complexes $Cp_3U(\eta^2\text{-}N_2C_3H_3)$ ($N_2C_3H_3$ = pyrazolyl) [56] and $Cp_3U(\eta^2\text{-}COCHP(C_6H_5)_2CH_3)$ [57] confirm the stability of such side-on derivatives even in the crystalline state, provided that the η^2-coordinated ligand does not cause severe steric congestion with the Cp-ligands.

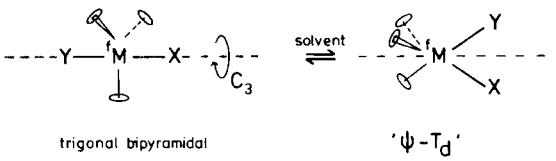

Fig. 21. Possible isomerization equilibrium of $[Cp_3UXY]^q$-species.

In solution other systems have been observed [20, 58] or can be postulated as essential transient species [34, 59, 60]. Usually, the ring proton Δ^{iso}-values of ψ-T_d-shaped $Cp_3U(\eta^1\text{-}X)$-systems occur at room temperature between 9 and 10 ppm, while in case of a η^2-coordinated extra ligand Δ^{iso}-values between 18 and 20 ppm have been reported [56, 57, 60]. The Cp ring–proton Δ^{iso}-*vs*-T^{-1} plots of the most recently described [60] products $Cp_3U(COR)$ that have been obtained by CO-insertion into Cp_3UR-systems (Cp = C_5H_5 and R = alkyl groups), and involve most probably an η^2-COR ligand, are again strictly linear and reminiscent of the Curie–Weiss rule.

Although it seems doubtful that a clean Δ^{iso}-*vs*-T^{-1} diagram of an authentically trigonal bipyramidal $[Cp_3UXY]^q$-system has yet been observed, its room temperature Δ^{iso} can, from the appearance of most of the plots of Figs. 19 and 20, be guessed as being less than 10 ppm. Thus equilibrium mixtures of rapidly interconverting isomers with *trans*- and *cis*-coordinated ligands X and Y can, in cases of markedly temperature-dependent molar ratios, in fact be expected to display Δ^{iso}-*vs*-T^{-1} plots of unusual shapes. Considering the usually widely differing Δ^{con}-values of the α- and β-ring H-atoms of ψ-T_d-shaped complexes with rapidly rotating C_5H_4R-ligands ($\Delta\Delta^{con} \approx 40$ ppm at 300 K), the corresponding very small $\Delta\Delta^{con}$-values of dissolved $[(MeCp)_3UXY]^-$-systems ($\leqslant$3 ppm) may suggest more intrinsic changes of the metal-to-ring bonding than just a reduction of the angle 'MeCp' UX ('MeCp' = ring centre) from *ca.* 100 (for ψ-T_d) to 90 degrees (for tbp). One possible explanation might be based on the assumption of very rapid changes of the MeCp ring hapticity accompanied by equally rapid intramolecular pseudorotations of the partially coordinated MeCp- (or Cp-) ligand, *e.g.* schematically

$$(\eta^5\text{-}C_5H_4R)_3UXY \rightleftharpoons (\eta^5\text{-}C_5H_4R)_2(\eta^3\text{-}C_5H_4R)UXY \rightleftharpoons (\eta^5\text{-}C_5H_4R)_2(\eta^1\text{-}C_5H_4R)UXY \quad (13)$$
$$\rightleftharpoons \ldots \text{ etc.}$$

Informative observations in this context are that (a) according to Figs. 19 and 20 the dissolved anionic complexes $[Cp_3U(NCS)_2]^-$ and $[MeCp_3U(NCS)]^-$ display the largest Δ^{iso}-values, suggesting a particularly large amount of isomer *2* (of Fig. 21) in equilibrium; (b) that NCS^- is a much 'stronger' ligand than *e.g.* $NCBH_3^-$ (which latter ligand is immediately substituted by NCS^-), and (c) that nevertheless two Cp-ligands may be replaced by NCS in the presence of NCS-ions in excess, and $[K, 222]^+$ as the countercation, to give the novel $[CpU(NCS)_5]^{2-}$-dianion [61] ('222' being a cryptand ligand).

Magnetic Anisotropy and CF-splitting of Uranocene

Although the sandwich-type molecule $(\eta^8\text{-}C_8H_8)_2$-U(IV) represents the most symmetric organo-f-element complex known, the electronic structure of this $[Rn]5f^2$-system is still not fully understood [73]. In terms of CF-theory, the nature of the electronic ground state and of the four next-following CF-states may be classified by the quantum numbers J_z = 0, ±1, ±2, ±3 and ±4 originating from the ground manifold $^3H_4$ of the spheric U(IV)-ion. So far it has not been possible to determine by purely theoretical means which particular set of CF-splitting parameters $\{B_2^0, B_4^0$ and $B_6^0\}$ would provide the most realistic sequence, at least of the lowest CF-states.

In spite of detailed studies both of the NIR/VIS absorption- and MCD-spectra, three independent pieces of information allowing unambiguous estimates of the three B_n^0-parameters could not be obtained. It appears, however, that two electronic Raman transitions are observable, one at 466 cm^{-1} which has been assigned to the excitation from the ground state to the first excited state [62], and a

second transition at 2330 cm^{-1} [63], most probably attributable to the third excited CF-state. It is tempting to correlate these data with the known magnetochemical properties of uranocene and its derivatives, hopefully to arrive at a realistic CF-splitting pattern.

Combining, in the sense of Scheme 2, the known temperature dependence of $\bar{\chi}$ of $(C_8H_8)_2U$ [64] and of $\chi_{\parallel} - \chi_{\perp}$ of the derivative $(C_8H_7SiMe_3)_2U$ [9], and adopting here the relation: $\mu^2 = 8.00 \cdot \chi \cdot T$, the various μ^2(exp.)-*vs*-T plots of Figs. 22 to 24 have been obtained [63]. Orbital reduction parameters were chosen such that at 250 K complete agreement of μ^2(exp.) and μ^2(calc.) resulted. The corresponding μ^2(calc.)-*vs*-T plots result from three separate model calculations in which an optimal fitting of the various μ^2(exp.)- and μ^2(calc.)-*vs*-T curves has been attempted. As previous experience with the CF-treatment had suggested that the CF-parameter B_6^0 might be negligibly small (as compared with B_4^0 and B_2^0), all three calculations are based on the assumption: $B_6^0 = 0$.

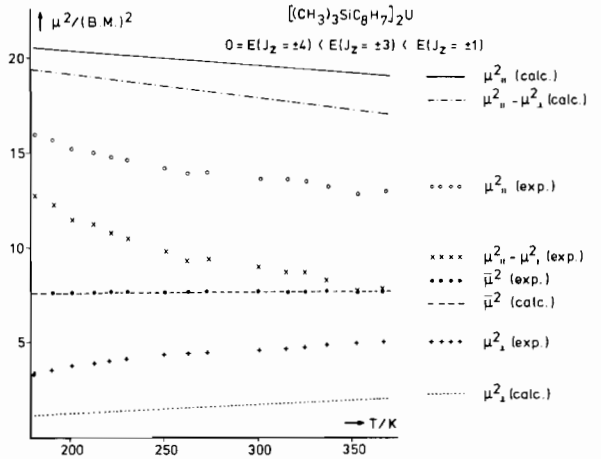

Fig. 22. μ^2-*vs*-T diagrams (comparison of μ(exp.)^2- and μ(calc.)^2-values) of $C_8H_7SiMe_3)_2U$. Assumed sequence of CF-states: $E(J_z = \pm 4) < E(J_z = \pm 3) < E(J_z = \pm 1) < \ldots$ etc..

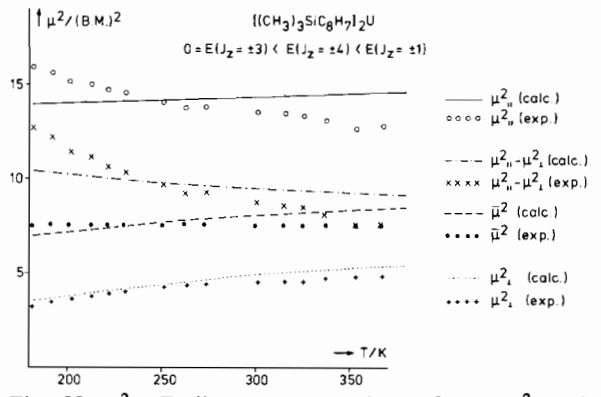

Fig. 23. μ^2-*vs*-T diagrams (comparison of μ(exp.)^2- and μ(calc.)^2-values) of $(C_8H_7SiMe_3)_2U$. Assumed sequence of CF-states: $E(J_z = \pm 3) < E(J_z = \pm 4) < E(J_z = \pm 1) < \ldots$ etc..

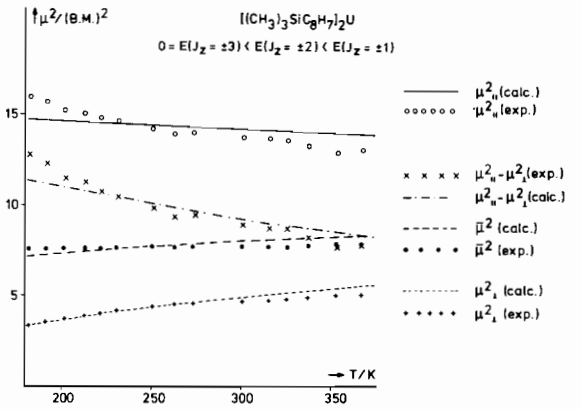

Fig. 24. μ^2-*vs*-T diagrams (comparison of μ(exp.)^2- and μ(calc.)^2-values) of $(C_8H_7SiMe_3)_2U$. Assumed sequence of CF-states: $E(J_z = \pm 3) < E(\pm 2) < E(J_z = \pm 1) < \ldots$ etc..

It is quite instructive that while $\bar{\chi}^2$(exp.) and $\bar{\chi}^2$-(calc.) can be fitted equally well in all three cases, the attempt to fit the other quantities too has been successful only for the sequence

$$0 = E(J_z = \pm 3) < E(J_z = \pm 2) < E(J_z = \pm 1) < \ldots \text{etc.}$$

with $E(J_z = \pm 2) = 466\ cm^{-1}$; $E(J_z = \pm 1) = 2330\ cm^{-1}$.

The alternative sequence that would likewise fulfill the selection rules of Raman spectroscopy: $0 = E(Jz = \pm 3) < E(J_z = \pm 4) < E(J_z = \pm 1) < \ldots$ etc., can, in view of the assumptions underlying the calculation, not fully be discarded; however, the agreement of some experimental and calculated quantities ($\mu_{\parallel}^2$ and $\mu_{\parallel}^2 - \mu_{\perp}^2$) becomes not only poor toward very low temperatures, but again above room temperature. No satisfactory agreement is, however, achieved for the assumed sequence: $0 = E(J_z = \pm 4) < E(J_z = \pm 3) < E(J_z = \pm 1) < \ldots$ etc. It must also be admitted that some improvement of the actual magnetic anisotropy of uranocene may be expected from the preparation, and appropriate assessment of the NMR-spectra, of different derivatives involving more rigid ring substituents than a $SiMe_3$-group [8]. It will be difficult to make sure that a ring substituent that is optimally suited for the determination of a relevant G-value does not simultaneously delete the axial symmetry of the magnetic susceptibility tensor.

Estimation of the Contact Shift Contribution, Δ^{con}

The calculated Δ^{con}-values of the Cp-ring H-atoms of the adducts $[Cp_3LnNCBH_3]^-$ are all positive for Ln = Pr and Nd, the ratio $\Delta^{con}(Nd)/\Delta^{con}(Pr)$ agreeing approximately with the theoretical prediction by Golding and Halton [10(b)] for the 'high-temperature approximation'. It is noteworthy that both Δ^{iso} and Δ^{con} of the ring H-atoms have opposite signs, but are

TABLE X. Δ^{iso}(exp.)-, Δ^{dip}(calc.)- and Δ^{con}(calc.)-values (in ppm, room temp.) of the Cp-ring H-atoms of Various $Cp_3U^{IV}X$- and $[Cp_3LnL]^-$-systems.

Ligand X	Δ^{iso}(exp.)[a]	Δ^{dip}(calc.)[b]	Δ^{con}(calc.)
n-C_4H_9	9.06	$\leqslant -17.69$	$\geqslant 26.75$
$H_3BC_2H_5$	12.8	−10.26	23.06
C_5H_5	19.96	0	19.96
Cl[c]	9.40	6.81	2.59
Cl[d,f]	29; −10	22; −23	+7; +13
O(n-C_4H_9)	23.86	12.65	11.21
OC_2H_5[e]	18.0; 29.0	12.65	5.35; 16.35
$[Cp_3PrNCBH_3]^-$	−6.7	−17.88	11.18
$[Cp_3NdNCBH_3]^-$	3.7	−11.95	15.65
$(C_5H_4CH_3)_3PrCNCMe_3$	−19.3; −4.8	−17.88	−1.42; +13.08

[a] Data from refs. [8, 44] and the present work. [b] Calculation based on the $(\chi_{\parallel} - \chi_{\perp})$-values of Table VI ($\bar{G} = -8.0 \cdot 10^{21}$ cm^{-3}). [c] $(\chi_{\parallel} - \chi_{\perp})$-value of Table VI applied on $(C_5H_5)_3UCl$. [d] Observed and calculated data of ref. [44]. [e] Experimental data from ref. [55] (30 °C). [f] With C_5H_4R-ligands.

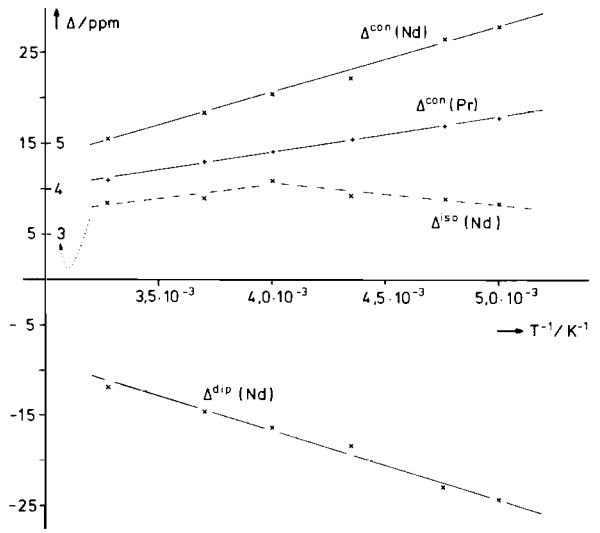

Fig. 25. Δ-*vs*-T^{-1} plots of $[Cp_3Ln(NCBH_3)]$ (Ln = Pr or Nd). Note different Δ-scale for Δ^{iso}(Nd).

proportional to T^{-1}, while the directly observable quantity Δ^{iso} is almost temperature-independent and passes a shallow maximum (Fig. 25).

As expected, the Cp ring-H Δ^{con}-values of corresponding $4f^2$- and $5f^2$-systems of the most general type Cp_3^fMX are both positive and of comparable magnitude. The room temperature data listed in Table X must, however, be considered as rough estimates as their reliability may be limited by the assumptions underlying the determination of Δ^{dip}. Nevertheless, it seems that in the case of the Cp_3UX-systems Δ^{con} varies noticeably with the nature of the ligand X, which might suggest some complexity in the 'mechanism' of the transfer of free spin density onto the ring protons. It is also surprising that Δ^{con} of the $5f^2$-complexes does not markedly exceed Δ^{con} of homologous $4f^2$-systems.

In the case of the binuclear complexes $[Cp_3Ln(\mu\text{-}NCBH_3)LnCp_3]^-$ (Fig. 8), the contact contribution $\Delta^{con}(B\underline{H}_3)$ of the three equally bridging H-atoms of the BH_3-group may also be estimated under the assumption that both Cp_3Ln-moieties display the same magnetic anisotropy $\chi_{\parallel} - \chi_{\perp}$ as in mononuclear Cp_3LnL. For Ln = Pr, $\Delta^{iso}(B\underline{H}_3)$ at room temperature is approximated by eqn. 14

$$\Delta^{iso}(exp.) = \Delta_1^{dip} + \Delta_2^{dip} + \Delta_1^{con} = 160 \text{ ppm} \quad (14)$$

where Δ_1^{dip} and Δ_2^{dip} are the contributions to the total dipolar shift by the η^3-H_3B- and N-coordinated Cp_3Pr ($\Delta_2^{dip} \approx 25$ ppm), respectively. Adopting $G = 1.01 \cdot 10^{23}$ cm^{-3} [33] for the bridging H-atoms, Δ_1^{dip} will amount to +226 ppm, and Δ^{con} finally arrives at −90 ppm. This latter value is of the same sign, but somewhat larger in magnitude, than the Δ^{con}-value evaluated for the η^3-H_3B-group of the $5f^2$-system $Cp_3U(\eta^3\text{-}H_3BC_2H_5)$ which lies around −60 ppm [33]. It must be recalled that the latter complex is not involved in any rearrangement equilibrium, while for the binuclear Pr-complex (at least at room temperature) rapid interchange of the Cp_3Pr-moieties must be accounted for (eqn. 7).

Negative Δ^{con}-values are commonly observed for nuclei of atoms directly bonded to paramagnetic metal ion of the configurations f^2 and f^3. For instance, negative Δ^{con}-contributions between −100 and −200 ppm have been suggested from the observed ^{13}C-NMR shifts of the Cp-ring C-atoms of Cp_3UX-systems (X = BH_4 or Cl [9,44, 69]) and Cp_3Pr [31], as well as for the ^{11}B-NMR shift of Cp_3UBH_4 (*ca.* −240 ppm [9]). An exceedingly negative Δ^{con}-value may be expected for the directly coordinated H-atoms of the dissolved compound $[Cp_2^*UH_2]_2$ (Cp^* = C_5Me_5; Δ^{iso} = −316.8 ppm [65]) in which the H-atoms oscillate rapidly between terminal and bridging positions, being thus on average subjected to more than one paramagnetic ion.

Conclusions

Principally, information of relevance for the electronic structure of a paramagnetic f-element compound is contained both in the dipolar and in the contact contribution of its isotropic NMR shifts. However, for the time being, access to substantial deductions appears more facile from the former, but will in general not prove satisfactory until an optimal combination with complementary analytical techniques is achieved. It is also imperative to check each NMR-sample first (mainly by NMR) for its molecular structure in solution, and incidentally its reactivity. Thus even the precisely determined molecular structures of crystalline $(C_5H_5)_3LnCNC_6H_{11}$-complexes (Ln = Pr and Ho [18]) are not fully identical with the appearance of the dissolved molecules. Likewise the complex $(C_5H_4CH_2C_6H_5)_3UCl$ must in solution not necessarily adopt its singular c_{3v}- conformation with non-rotating ring ligands as found by single crystal X-ray crystallography [70].

Rather unexpectedly, even the complex $(C_5H_4SiMe_3)_3Pr$ which appears to involve non-rotating ring ligands in the absence of an extra ligand L, displays again ^1H NMR spectra indicative of freely rotating ring ligands in the presence of equimolar amounts of $[NBu_4^n][NCBH_3]$ and in CD_3CN-solution, respectively [31]. It should be recalled that certain extra ligands L (or X) force the three Cp-rings to adopt positions more remote from the metal ion than in the case of sterically less demanding ligands (*e.g.* Cp_4U: U–C = 281ppm; Cp_3UCl: U–C = 273 ppm [71]). There is, moreover, ^1H NMR spectroscopic evidence of η^5-coordination of all four $C_5H_4CH_3$-ligands in $(C_5H_4CH_3)_4U$ in that the ring H-atoms give rise to 4–5 relatively sharp and close-lying resonances between 20.0 and 22.5 ppm [55].

On the other hand, structurally well-investigated complexes that are not expected to alter their shape in solution should be subjected to more sophisticated NMR-assessments even when they are devoid of axial (and cubic) symmetry. Only in the case of unequivocal evidence that rapid rearrangement equilibria interfere with the verification of one singular, structurally well-determined species, NMR-studies will not lead to electronically relevant results. For instance, the salt-like complexes of the type $[M]^+[Cp_3UXY]^-$ (M = organic cation) involve the structurally well-determined anion only in the crystalline state, and the only way to arrive at its magnetic anisotropy would be via laborious magnetic susceptibility studies of carefully oriented single crystals.

Acknowledgements

This work has been supported by the Deutsche Forschungsgemeinschaft (D.F.G.) and the Fonds der Chemischen Industrie. The authors appreciate the valuable assistance by Dr. E. Haupt, Dr. V. Pank and Mr. K. Kühne in NMR-spectroscopy problems. Profs. P. Zanella and G. de Paoli have kindly furnished us with samples of the complexes $(C_5H_4R)_2U(BH_4)_2$ (R = CH_3 and $Si(CH_3)_3$. R.D.F. and H.-D.A. also thank Prof. B. Kanellakopulos for many valuable discussions.

References

1 J. A. Konigstein, *Mol. Spectrosc., 4,* 196 (1976); V. T. Aleksanian, G. K. Borisov, G. G. Devyatych, B. F. Gächter, J. A. Konigstein and B. E. Schneider, *J. Raman Spectrosc., 2,* 345 (1974).
2 H.-D. Amberger, W. Grape and E. Stumpp, *J. Less Common Metals, 95,* 181 (1983).
3 A. K. Banerjee, R. W. Schwartz and M. Chowdury, *J. Chem. Soc., Faraday Trans. II, 77,* 1635 (1981) and literature therein.
4 (a) W. DeW. Horrocks, Jr. and J. P. Side III, *Science, 177,* 994 (1972); S. P. Chachra and A. Mookheji, *Ind. J. Pure Appl. Phys., 7,* 559 (1962). (b) E. Ellis, *Chem. Phys. Lett., 1,* 80 (1967), and references therein.
5 For some recent reviews in this field, see: J. Reuben, *Progr. NMR Spectrosc., 9,* 1 (1979); C. M. Dobson and B. A. Levine, in 'New Techniques in Biophysics and Cell Biology', R. H. Pain and B. E. Smith, eds., Vol. 3, p. 19, J. Wiley, New York, 1976; F. Inagaki and T. Miyazawa, *Progr. NMR Spectrosc., 47,* 67 (1981).
6 See *e.g.* J. P. Jesson, in 'NMR of Paramagnetic Molecules', G. N. La Mar, W. DeW. Horrocks, Jr. and R. H. Holm, Academic Press, New York and London, 1973, p. 1.
7 See *e.g.* W. DeW. Horrocks, Jr., in 'ESR and NMR of Paramagnetic Species in Biological and Related Systems', I. Bertini and R. S. Drago, D. Reidel Publ. Comp., Dordrecht, Holland, (1979), p. 55; see also Refs. [8] and [9].
8 W. D. Luke and A. Streitwieser, Jr., 'ACS Symp. Ser. 131', N. M. Edelstein, Washington, D.C., p. 93, 1980.
9 R. D. Fischer, in 'Organometallics of the f-Elements', T. J. Marks and R. D. Fischer, D. Reidel Publ. Comp., Dordrecht, Holland, p. 337, 1979.
10 (a) L. C. Stubbs and B. McGarvey, *J. Magn. Resonance, 50,* 249 (1982); R. J. Booth and B. McGarvey, *ibid., 36,* 7 (1979) and further references therein; (b) R. M. Golding and M. P. Halton, *Aust. J. Chem., 25,* 2577 (1972).
11 D. F. Evans, *J. Chem. Soc. (London),* 2003 (1959); J. Löliger and R. Scheffold, J. Chem. Educ., 49, 646 (1972); D. Ostfeld and I. A. Cohen, *ibid., 49,* 829 (1972).
12 A comprehensive survey of the literature up to mid-1978 is given in ref. [9].
13 Throughout this contribution, 'rapid' is understood in terms of 'rapid on the ^1H NMR time-scale'.
14 R. v. Ammon, R. D. Fischer and B. Kanellakopulos, *Chem. Ber., 104,* 1072 (1971).
15 R. v. Ammon and B. Kanellakopulos, *Ber. Bunsenges. Phys. Chem., 76,* 995 (1972).
16 R. v. Ammon and R. D. Fischer, *Angew. Chem. Internat. Edit., 11,* 675 (1972).
17 For the derivation of the geometry factor, see ref. [26] (a); applications are given *e.g.* in refs. [5–9] and [16].
18 J. H. Burns and W. H. Baldwin, *J. Organomet. Chem., 120,* 361 (1976).

19 See: R. v. Ammon, B. Kanellakopulos, R. D. Fischer and V. Formacek, *Z. Naturf. 28b,* 200 (1973), and ref. [15].
20 R. D. Fischer, R. v. Ammon and B. Kanellakopulos, *J. Organomet. Chem., 25,* 123 (1970); R. v. Ammon, personal communications.
21 L. Brun, *Acta Cryst., 20,* 739 (1966).
22 H.-D. Amberger and N. M. Edelstein, unpublished results.
23 H.-D. Amberger and N. M. Edelstein, *Abstr. 1st Int. Conf. Chem. Technol. Lanthanides and Actinides,* Sept. 5–10, 1983, Venice, Italy, p. 90 (B 22).
24 P. J. Stiles, *Mol. Phys., 27,* 501 (1974); P. J. Stiles and R. M. Wing, *J. Magn. Resonance, 15,* 510 (1974).
25 *Ca.* 34 mmol/l in CH_2Cl_2 as compared with 2 mmol/l in toluene [40].
26 (a) B. Bleaney, *J. Magn. Resonance, 8,* 91 (1972); (b) B. Bleaney, C. M. Dobson, B. A. Levine, R. B. Martin, R. J. P. Williams and A. V. Xavier, *Chem. Comm.,* 791 (1972).
27 R. M. Golding and P. Pyykkö, *Mol. Phys., 26,* 1389 (1973).
28 W. Wagner, *Doctoral Dissertation,* Universität Heidelberg, 1974.
29 S. Spiliadis and A. A. Pinkerton, *J. Chem. Soc., Dalton Trans.,* 1815 (1982).
30 A survey of various papers by Horrocks *et al.* on this subject is given in ref. [7]; see also ref. [27].
31 R. D. Fischer and W. Jahn, unpublished results.
32 T. J. Marks, A. M. Seyam and J. R. Kolb, *J. Amer. Chem. Soc., 95,* 5529 (1973).
33 T. J. Marks and J. R. Kolb, *J. Amer. Chem. Soc., 97,* 27 (1975).
34 L. Arnaudet, G. Folcher, H. Marquet-Ellis, E. Klähne, K. Yünlü and R. D. Fischer, *Organometallics, 2,* 344 (1983).
35 I. Bertini, C. Luchinat and E. Borghi, *Inorg. Chem., 20,* 303 (1981).
36 W. Hinrichs, D. Melzer, M. Rehwoldt, W. Jahn and R. D. Fischer, *J. Organomet. Chem., 251,* 299 (1983).
37 Li Xing-fu and R. D. Fischer, *Inorg. Chimica Acta, 94,* 50 (1983); Li Xing-fu and R. D. Fischer, manuscript in preparation.
38 J. H. Burns, W. H. Baldwin and F. H. Fink, *Inorg. Chem., 13,* 1916 (1974).
39 R. D. Fischer and W. Jahn, manuscript in preparation.
40 W. Jahn, *Doctoral Dissertation,* Universität Hamburg, 1983.
41 A. W. Spiegl, W. Havemann and R. D. Fischer, unpublished results, see also ref. [9].
42 J. L. Atwood, W. E. Hunter and H.-M. Zhang, *Inorg. Chimica Acta, 94,* 31 (1983).
43 A. Dormond, C. Duval-Huet and J. Tirouflet, *J. Organomet. Chem., 209,* 341 (1981).
44 G. Folcher, G. Langlet and P. Rigny, *Nouv. J. Chim., 7,* 245 (1983).
45 R. D. Fischer, E. Klähne and J. Kopf, *Z. Naturf., 33,* 1339 (1978).
46 G. Bombieri, F. Benetollo, E. Klähne and R. D. Fischer, *J. Chem. Soc., Dalton Trans.,* 1115 (1983).
47 G. Bombieri, F. Benetollo, K. W. Bagnall, M. J. Plews and D. Brown, *J. Chem. Soc., Dalton Trans.,* 45 (1983).
48 K. W. Bagnall, M. J. Plews, D. Brown, R. D. Fischer, E. Klähne, G. W. Landgraf and G. R. Sienel, *J. Chem. Soc., Dalton Trans.,* 1999 (1982).
49 R. D. Fischer and K. Yünlü, unpublished results.
50 Subsequently, corresponding complexes have also been obtained with Ln = Ce–Nd: Li Xing-fu, C. Apostolidis, W. Jahn, B. Kanellakopulos and R. D. Fischer, manuscript in preparation.
51 (a) R. G. Hayes and J. L. Thomas, *Organomet. Chem. Rev., A7,* 1 (1971); (b) C. M. Aderhold, *Doctoral Dissertation,* Universität Heidelberg, 1974; (c) B. Kanellakopulos, personal communication.
52 R. D. Fischer, E. Klähne and G. R. Sienel, *J. Organomet. Chem., 238,* 99 (1982).
53 R. D. Fischer, K. Yünlü, W. Jahn, H.-D. Amberger and B. Kanellakopulos, *13èmes Journées des Actinides,* Elat/Israel, Apr. 26–28, 1983, Abstr. D3.
54 R. D. Fischer and K. Yünlü, *Z. Naturf., 38b,* 166 (1983).
55 R. v. Ammon, personal communication, see also ref. [20].
56 C. W. Eigenbrot and K. N. Raymond, *Inorg. Chem., 20,* 1553 (1981).
57 R. E. Cramer, R. B. Maynard, J. C. Paw and J. W. Gilje, *Organometallics, 1,* 869 (1982).
58 V. K. Vasil'ev, V. N. Sokolov and G. N. Kondratenkov, *Doklady Akad. Nauk. SSSR, 236,* 518 (1977).
59 V. K. Vasil'ev, V. N. Sokolov and G. N. Kondratenkov, *J. Organomet. Chem., 142,* C7 (1977).
60 G. Paolucci, R. Rossetto, P. Zanella, K. Yünlü and R. D. Fischer, *J. Organomet. Chem.,* in press.
61 Li Xing-fu, R. D. Fischer, K. W. Bagnall, E. Klähne and G. R. Sienel, unpublished work.
62 R. F. Dallinger, P. Stein and T. G. Spiro, *J. Amer. Chem. Soc., 100,* 7865 (1978).
63 H.-D. Amberger, personal communication; H.-D. Amberger, *16th Rare Earth Research Conference,* Tallahassee, Florida, Apr. 18–21, 1983, Abstr. S9.
64 H.-D. Amberger, R. D. Fischer and B. Kanellakopulos, *Theoret. Chim. Acta, 37,* 105 (1975).
65 T. J. Marks, personal communication.
66 Y. Hristidu, *Doctoral Dissertation,* Universität München, 1962.
67 H.-D. Amberger, R. D. Fischer and B. Kanellakopulos, *Z. Naturf., 31b,* 12 (1976).
68 B. Kanellakopulos, *Habilitationsschrift,* Universität Heidelberg, 1972.
69 E. Fukushima and S. D. Larsen, *Chem. Phys. Letters, 44,* 285 (1976).
70 J. Leong, K. O. Hodgson and K. N. Raymond, *Inorg. Chem., 12,* 1329 (1973).
71 See: K. N. Raymond, in ref. [9], p. 249.
72 E. Fukushima, in 'Proceed. 18th Ampère Congr'., P. S. Allen, E. R. Andrew and C. A. Bates, Nottingham, England, 1974, p. 239.
73 For a most recent, quasi-relativistic MO-treatment see: N. Rösch, *Inorg. Chim. Acta, 94,* 83 (1983).